Soil Biology and Biochemistry 191 (2024) 109343

Contents lists available at ScienceDirect

Soil Biology and Biochemistry

journal homepage: www.elsevier.com/locate/soilbio

Preceding crop legacy modulates the early growth of winter wheat by influencing root growth dynamics, rhizosphere processes, and microbial interactions

Nikolaos Kaloterakis [a,*], Mehdi Rashtbari [b], Bahar S. Razavi [b], Andrea Braun-Kiewnick [c], Adriana Giongo [c], Kornelia Smalla [c], Charlotte Kummer [a], Sirgit Kummer [a], Rüdiger Reichel [a], Nicolas Brüggemann [a]

[a] Institute of Bio- and Geosciences, Agrosphere (IBG-3), Forschungszentrum Jülich GmbH, 52428 Jülich, Germany
[b] Department of Soil and Plant Microbiome, Institute for Phytopathology, Christian-Albrechts-University of Kiel, 24118, Kiel, Germany
[c] Institute for Epidemiology and Pathogen Diagnostics, Julius Kühn Institute (JKI) – Federal Research Centre for Cultivated Plants, 38104, Braunschweig, Germany

A B S T R A C T

Successive winter wheat (WW) rotations are associated with a substantial yield decline, and the underlying mechanisms remain elusive. An outdoor experiment was set up using sandy loam soil. WW was grown in rhizotrons, in soil after oilseed rape (KW1), after one season of WW (KW2), and after three successive seasons of WW (KW4). We applied zymography and harvested the plants at the stem elongation stage to observe changes in the activity of β-glucosidase (BGU) and leucine aminopeptidase (LAP), as well as using glucose (GLU) imaging to observe glucose release patterns in the rhizosphere of WW. Several biochemical and microbial properties of the bulk soil and the rhizosphere of the rotational positions were measured. KW2 and KW4 exhibited reduced plant biomass compared to KW1. There was a higher root length density and root mean diameter as well as a lower specific root length for KW1 compared to KW2 and KW4. KW1 soil had a lower mineral N concentration and microbial biomass carbon (C) and nitrogen (N) than KW2 and KW4, which translated to a lower plant C:N ratio. A greater rhizosphere extent of BGU and LAP across the soil profile was also visible for KW1 compared to KW2 and KW4 using zymography. Lower dissolved organic C and hotspot areas of GLU in the rhizosphere of successive WW might explain shifts in the microbial community composition, possibly leading to a dysbiosis with the soil microbes in the rhizosphere. Soil depth and rotational position explained most of the variance in the soil microbial communities. The relative abundance of *Acidobacteriota*, *Gemmatimonadota*, *Nitrospirota*, and *Chloroflexi* significantly varied among the rotational positions. Our results highlight the effect of WW rotational positions on soil and plant properties, as well as microbial community dynamics, and provide evidence for the pathways driving biomass decline in successively grown WW.

1. Introduction

Due to its high economic importance, higher proportions of winter wheat (WW) are added to crop rotations by growing two or more WW crops after a break crop (Kwak and Weller, 2013). The positive effects of adding non-cereal break crops to the rotation have been well established. On a global scale, up to 40 % of the cultivated wheat is grown successively, with only a late summer fallow as a break (Angus et al., 2015; Yin et al., 2022). However, growing WW successively in the same field increases the risk of soil-borne infections, such as the take-all disease caused by *Gaeumannomyces graminis* var *tritici* (Ggt, recently re-named *Gaeumannomyces tritici*), which is the most important soil-borne fungal pathogen of WW, causing root rotting and significant yield losses (Cook, 2003; Kwak and Weller, 2013). Plant yield is negatively affected by the self-succession of wheat in the same field (Sieling and Christen, 2015) due to the increased incidence of Ggt (Smagacz et al., 2016). The take-all disease persists in wet and dry conditions and can cause a yield decline of up to 50 % (Palma-Guerrero et al., 2021). However, it has been recently demonstrated that the yield reduction is evident in a dry year with no obvious Ggt infection (Arnhold et al., 2023a). Adding non-cereal break crops to the rotation, such as oilseed rape, has been shown to enhance the yield of the following WW (Angus et al., 2015; Weiser et al., 2018). Nevertheless, the complex interactions between pre-crop plants and microorganisms in the rhizosphere remain unclear.

WW allocates 20–30 % of the assimilated carbon (C) belowground through the root (Kuzyakov and Domanski, 2000), known as rhizodeposition. Rhizodeposition shapes a dynamic and heterogeneous microenvironment in the rhizosphere, which is estimated to extend between 0.5 mm and 4 mm for different plant species (Kuzyakov and Razavi,

* Corresponding author.
E-mail address: n.kaloterakis@fz-juelich.de (N. Kaloterakis).

https://doi.org/10.1016/j.soilbio.2024.109343
Received 28 July 2023; Received in revised form 23 January 2024; Accepted 27 January 2024
Available online 6 February 2024

2019) and to be governed by mutualistic, parasitic, and neutral interactions between roots and soil microorganisms (Pausch and Kuzyakov, 2017). Root exudates are a highly influential pool of organic compounds with a low molecular weight, referred to as rhizodeposits, which are secreted into the rhizosphere. They provide a nutrient source for soil microbes, stimulating their activity, but also acting as signals for both mutualists and parasites, with consequences for plant health (Hernández-Calderón et al., 2018; Mohan et al., 2020). The efflux of primary metabolites to the soil due to root exudation creates a plant C source, which fuels microbial growth and nutrient mineralization, affecting plant performance and health. Soil microbes, in turn, influence root exudation by producing extracellular enzymes and polymeric substances (Costa et al., 2018; Korenblum et al., 2020). Both processes require significant amounts of energy and are therefore an investment from both the plant and microbial sides to stimulate their nutrient acquisition as well as proliferation in the soil (Costa et al., 2018; Canarini et al., 2019). For plants, this can be exhibited as the stimulation of root growth. Plants also excrete secondary metabolites (e.g. flavonoids) into their rhizosphere in response to biotic stress and herbivores to induce systemic resistance (ISR; Vlot et al., 2020; Pang et al., 2021). Labile soil organic matter (SOM) and nitrogen (N) mineralization following enhanced enzymatic activity (e.g. protein and cellulose-degrading enzymes) are thus mediated by root exudation and indirectly increase plant nutrient uptake (Meier et al., 2017). These interactions can induce changes in the root system architecture and, in turn, influence nutrient and water uptake (Galloway et al., 2020).

WW shapes its rhizosphere microbial community through rhizodeposition (Wen et al., 2022), enhancing nutrient uptake and plant performance. In particular, oilseed rape and legumes as preceding crops have been associated with the selection of beneficial microbial taxa, and the suppression of pathogenic microbial taxa, in WW (Vujanovic et al., 2012). This is mainly due to differences in the residue quality that affect its decomposition process (Kerdraon et al., 2019). WW residues mainly contain cellulose and have a higher lignin content than oilseed rape, decelerating their decomposition rate (Pascault et al., 2010). In addition to the soil legacy effect of the residues of the preceding crop, glucose release in the rhizosphere of the growing WW, which is affected by root growth and functioning, can shape microbial communities and, therefore, affect the productivity of WW (Qi et al., 2022). Glucose is the most abundant monosaccharide in the root exudates of WW (Yahya et al., 2021) and is a readily available C source for the soil microbiome. As such, it can fuel both mutualistic, competitive, and pathogenic interactions between soil microorganisms and plants that might affect plant productivity (Philippot et al., 2013). Besides root pathogens that can directly affect plant health, such as Ggt, the prevalence of other detrimental microorganisms in the rhizosphere can compete with roots for available nutrients (Kuzyakov and Xu, 2013). This leads to reduced root growth and exudation, which further increases the C cost for the soil microbial community, creating negative plant–soil feedback (Cortois et al., 2016; Bennett and Klironomos, 2019). Diversified WW rotations with oilseed rape as a preceding crop are known to increase WW yield compared to successively grown WW (Kirkegaard et al., 2008; Ramanauskienė et al., 2018). Most studies show a positive effect on WW pathogen suppression, soil structure, and a high residual N content after oilseed rape harvest (Sieling and Christen, 2015; Weiser et al., 2018; Hilton et al., 2018), although these positive effects have not always been consistently observed (Arnhold et al., 2023b).

Our study aimed to investigate the underlying mechanisms that govern the productivity of WW grown in self-succession as opposed to WW grown after a break crop, such as oilseed rape. Specifically, we focused on the quantification of root growth parameters and the associated biochemical parameters (C and N translocation) as well as on the microbial (bacterial and archaeal) compositions in the rhizosphere (RH) and bulk (BS) soil of WW grown in different rotational positions. We hypothesized that there would be reduced rhizodeposition in self-successional WW, resulting in distinct changes in the microbial community composition and reduced production of hydrolytic enzymes. The reduced rhizodeposition in self-successional WW would be followed by changes in the microbial community composition and a decreased microbial activity, influencing nutrient (especially mineral N) uptake by the plant and plant biomass.

To test these hypotheses, an outdoor rhizotron experiment was conducted, contrasting three rotational positions of WW. We combined zymography and glucose (GLU) imaging on WW at the onset of stem elongation to observe changes in the activity of two important C- and N-acquiring enzymes, β-glucosidase (BGU), and leucine aminopeptidase (LAP) as well as glucose release in its rhizosphere. We also combined soil biochemical and microbiome analyses to assess nutrient and C availability as well as microbial community composition in the rhizosphere of WW and to understand the mechanisms underlying WW performance in those rotational positions.

2. Methods

2.1. Experimental design

The soil was collected in September 2021 from the experimental farm Hohenschulen, Faculty of Agricultural and Nutritional Sciences, Kiel University, 54°19′05″N, 9°58′38″E, Germany. The crop rotation trial was established in 1989. It included the following factors: a) rotational position (oilseed rape, first wheat after oilseed rape, third wheat grown continuously), b) WW varieties (4 levels), and c) N fertilization levels (4 levels). Composite soil samples for rhizobox experiments were taken from oilseed rape (KW1), first wheat plots (KW2), and third wheat plots (KW4) (N = 4 replications) containing the WW cultivar "Nordkap" (SAATEN-UNION GmbH, Isernhagen, Germany) and optimal N fertilization (240 kg N ha^{1}). Soil was collected from the topsoil (0–30 cm) and subsoil (30–50 cm) and sieved to 2 mm. The residues of the preceding crop were not removed from the soil before sampling, and the field was ploughed after sampling. The crop rotations are referred to as rotational positions hereinafter. After the harvest of the different preceding crops, the plant residues remained on the field. The soil is a Cambic Luvisol of sandy loam texture (44 % sand, 35 % silt, and 21 % clay; Sieling, 2005). The lack of effervescence in our soil samples after adding 10 % HCl indicated the absence of carbonates, which was confirmed by an average $\delta^{13}C$ value of −26.92 ‰ of soil samples analyzed before the start of the experiment. Table 1 shows some important initial soil biochemical parameters specific to the three rotational positions.

We conducted an outdoor rhizotron experiment (May 4, 2022 to June 30, 2022) using newly designed rhizotrons with a height of 100 cm, a width of 35 cm, and an inner thickness of 2.5 cm (Reichel et al., 2022). Each rhizotron was wrapped in a 50-mm-thick, aluminum-coated Rockwool foil to reduce soil temperature fluctuations inside the rhizotron. Bulk density was adjusted to 1.35 g cm^{-3} and deionized water was added to adjust soil moisture to 70 % water-holding capacity (215 g H_2O soil kg^{-1}) at the onset of the experiment. The plants were subsequently rain-fed throughout the experiment. The rhizotrons were placed on the campus of Forschungszentrum Jülich, Germany. All rhizotrons were consistently inclined at 45° to facilitate root growth along the lower side of the rhizotrons. WW seeds (cultivar "Nordkap") were germinated on petri dishes with sterile filter paper for 24 h in the dark at 23 °C. One germinated seed was subsequently sown into each rhizotron. The plants were not fertilized for the duration of the experiment. The plants were harvested at the stem elongation stage (BBCH 30).

2.2. Above and belowground plant growth analyses

The aerial plant parts were split at harvest into pseudostems (hereinafter referred to as stems) and leaves. The lower sides of the rhizotrons were then removed, and images of the root system along the soil profile were taken with a camera (DSLR Nikon D3500 Kit AF-P VR 18–55 mm, Nikon Corp., Tokyo, Japan). The soil profile was then divided into three

layers (0–30 cm, 30–60 cm, and 60–100 cm), and soil samples were taken from two soil compartments, i.e. RH sampled with microspatulas from ≤5 mm away from the rhizosphere of primary roots and root-free BS. We pooled and mixed subsamples to form a composite sample, and then split it into several parts to ensure sufficient soil was collected for every planned analysis. For analysis of microbial biomass C and N (C_{mic} and N_{mic}), we sampled root-affected soil from a distance between 5 mm and 20 mm away from the rhizoplane of primary roots. This measure was taken to ensure that a sufficient amount of soil (20 g per sample) was sampled to be used for this specific analysis. The roots were then retrieved after washing off the soil through a 1 mm sieve and stored in 30 % ethanol. They were scanned at 600 dpi (Epson Perfection V800 Photo, Epson, Japan) and analyzed with WinRhizo® software (Regent Instruments Inc., Quebec, Canada) for the following root growth traits: root length, average root diameter (R_{dia}), root surface area, and root volume. The roots were split into seven diameter classes: 0–0.05 mm, 0.05–0.1 mm, 0.1–0.5 mm, 0.5–1 mm, 1–1.5 mm, 1.5–2 mm, and ≥2 mm. Using these root growth traits, we computed the root length density (RLD), the specific root length (SRL), and the proportion of root length for the seven root diameter classes. Estimates of root tissue density (RTD) were made as described in Rose (2017). All plant materials were oven-dried at 60 °C to constant weight (maximum three days) to record their dry weight. Ball-milled (MM 400, Retsch, Germany) above and belowground plant samples, as well as soil samples, were weighed into tin capsules (HEKAtech, Wegberg, Germany) to determine the C and N content using an elemental analyzer coupled to an isotope-ratio mass spectrometer (EA-IRMS, Flash EA, 2000, coupled to Delta V Plus; Thermo Fisher Scientific Inc., Waltham, MA, USA).

2.3. Biochemical soil analyses

At harvest, soil samples were stored at −25 °C before analysis of mineral N, dissolved organic carbon (DOC), and total extractable nitrogen (TN). For the analysis, they were thawed and extracted using 0.01 M $CaCl_2$ (soil-to-solution ratio of 1:4 w:v), vortexed, shaken horizontally for 2 h at 200 rpm, centrifuged for 15 min at 690×*g*, and filtrated through 0.45 μm PP-membrane filters (Ø 25 mm; DISSOLUTION ACCESSORIES, ProSense B.V., Munich, Germany). Soil solution was stored overnight at 4 °C before DOC and TN analysis. Ammonium (NH_4^+) was measured by continuous-flow analysis (Flowsys, Alliance Instruments GmbH, Freilassing, Germany). Nitrate (NO_3^-) and sulfate (SO_4^{2-}) were measured by ion chromatography (Metrohm 850 Professional IC Anion – MCS, Metrohm AG, Herisau, Switzerland). Mg was measured by inductively coupled plasma optical emission spectroscopy (iCAP 6500; Thermo Fisher Scientific Inc., Waltham, MA, USA). The pH was measured in the same solution using a glass pH electrode (SenTix® 940, WTW, Xylem Analytics, Weilheim, Germany). DOC and TN were quantified with a total organic C (TOC) analyzer (TOC-V + ASI-V + TNM, Shimadzu, Japan). Using 0.01 M calcium acetate lactate (CAL) instead of $CaCl_2$ and following the same extraction protocol, the plant-available phosphorus (P_{CAL}) and potassium (K_{CAL}) were measured with inductively coupled plasma optical emission spectroscopy (ICP-OES, iCAP 6500; Thermo Fisher Scientific Inc., Waltham, MA, USA).

The chloroform-fumigation extraction (CFE) method was used to estimate microbial biomass C and N. Ten grams of fresh soil stored at 4 °C were weighed in beakers and placed inside a desiccator. They were incubated with ethanol-free chloroform (80 mL) at room temperature for 24 h. Soil samples were then extracted with 0.01 M $CaCl_2$ and analyzed with a TOC analyzer, as described previously. Non-fumigated soil samples were extracted using the same protocol. The difference between extracted C and N from fumigated and non-fumigated soil samples was used to calculate C_{mic} and N_{mic}, using the correction factors 0.45 and 0.4 as the extractable parts of C_{mic} (kEC) and N_{mic} (kEN), respectively (Wu et al., 1990; Joergensen, 1996).

2.4. Glucose imaging

Soil glucose imaging was applied to all rhizoboxes according to Hoang et al. (2022). Accordingly, phosphate powder (Sigma P7994) was dissolved in distilled water to make a 100 mL buffer solution with a concentration of 0.05 M (pH 7.4). Added to the solution were 1.7 unit/ml glucose oxidase from *Aspergillus niger* (Sigma G7141), 1.5 unit/ml peroxidase from horseradish (Sigma P8125), and 200 μM Ampliflu red (Sigma 90,101, Sigma-Aldrich, Darmstadt, Germany) dissolved in 60 μL dimethylsulfoxide. Installed rhizotrons were gently removed to avoid cutting roots. Polyamide membrane filters (pore size 0.45 mm – Tao Yuan, China) were cut into 10 × 20 cm strips. These membranes were saturated with the prepared reaction mixture solution before being attached to the rooted area. After 20 min of incubation (an optimal incubation time was tested in advance; time may differ between plant species (Hoang et al., 2022)), membranes were quickly removed, placed in a dark container, and immediately transferred to the dark room under UV light with a wavelength of 355 nm. The magenta-colored area on the membrane indicated glucose exudation as hydrogen peroxide generated from a reaction between glucose and glucose oxidase enzymes, which was catalyzed by horseradish peroxidase to convert colorless Ampliflu red into magenta-colored resorufin (Zhou et al., 1997).

2.5. Zymography

Zymography (BGU and LAP activity) was performed according to the protocol developed by Razavi et al. (2019). A 4-methylumbelliferyl-β-glucoside (MUF-β) and L-leucine-7-amino-4-methylcoumarin hydrochloride (AMC-L) (Sigma Aldrich, Germany) solutions were prepared in MES buffer ($C_6H_{13}NO_4SNa_{0.5}$, Sigma-Aldrich, Darmstadt, Germany) and TRIZMA ($C_4H_{11}NO_3 \cdot HCl$, $C_4H_{11}NO_3$, Sigma-Aldrich, Darmstadt, Germany), respectively, to make a fluorescent solution of 12 mM. The same polyamide membrane filters (Tao Yuan, China) with a pore size of 0.45 mm were selected to reduce enzyme diffusion through the pores (Razavi et al., 2016). The membranes were soaked in the fluorescent solution and then directly applied to the root-exposed side of the rhizoboxes before being subsequently covered with aluminum foil to avoid exposure to light and drying out. After 1 h of incubation, the membranes were quickly removed, cleaned with a soft brush, and exposed to UV light with an excitation wavelength of 355 nm in a dark room.

All images were taken with a digital camera (Canon EOS 6D, Canon Inc.) and a Canon lens EF 24–105 mm 1: 4 L IS II USM with the setting of aperture and shutter speed at f/5.6 and 1/10 s (for glucose imaging) and 1/8 s (for zymography), respectively. The calibration lines for glucose imaging were prepared by soaking a 4 cm^2 membrane in a glucose solution at respective concentrations of 0 mM, 2 mM, 4 mM, 6 mM, 8 mM, and 10 mM. The membranes were soaked in the respective reaction mixture solution in the same way as mentioned above. Fluorescent signals of glucose release on an area basis were calculated based on the volume of substrate solution taken up by a fixed membrane size.

Zymography processing was calibrated by soaking individual 4 cm^2 membranes in MUF solution at respective concentrations of 0 mM, 0.2 mM, 0.5 mM, 1 mM, 2 mM, 4 mM, 6 mM, 8 mM, and 10 mM. These membranes were exposed to UV light in the same way as the samples. Calibrated values were used to quantify the color intensity and to link BGU activity to the grey value. Fluorescent signals of MUF on an area basis were calculated based on the volume of substrate solution taken up by a fixed membrane size.

The image processing and analysis were conducted using the software package ImageJ. The hotspot percentage was calculated based on the pixel size proportion of the hot area to the entire image. In other words, hotspot areas were determined to have the 25 % higher pixel-wise enzyme activities after subtracting background values at zero concentration of the calibration line from all zymograms and glucose release images (Ma et al., 2018). Meanwhile, the rhizosphere extent of

each root was calculated from the root surface. The rhizosphere extent was determined for root segments for the following parameters: 1) glucose release and 2) BGU and leucine aminopeptidase activity (soil zymograms). To measure the rhizosphere extent, five horizontal transects (angle to the root ~90°) were randomly drawn across five randomly selected roots for the glucose release image and BGU zymogram using ImageJ. In total, this yielded 25 lines per image as pseudo-replicates, and their mean was used for each rhizobox (as a true replicate) (Bilyera et al., 2021).

2.6. Enzyme kinetics and turnover time

The kinetics of hydrolytic enzymes involved in C and N cycles were measured by fluorimetric microplate assays of 4-methylumbelliferone (MUF) and 7-amino-4-methyl coumarin (AMC) (Dorodnikov et al., 2009). A fluorogenic substrate based on MUF and one type based on AMC were used to assess enzymatic activities: 4-methylumbelliferyl-β-D-glucoside to detect BGU activity; L-Leucine-7-amino-4-methylcoumarin to detect LAP activity. All substrates and chemicals were purchased from Sigma-Aldrich (Darmstadt, Germany).

According to German et al. (2011), 1.0 g of soil was suspended in 50 mL of distilled water, of which 50 μL aliquots were pipetted into labeled wells of a 96-well microplate (Thermo Fisher, Denmark). A 50 μL buffer (MES/Trizma) and 100 μL respective substrate solution were then added to each well. The activity of enzymes was measured at three time points: 30 min, 60 min, and 120 min using CLARIOstar Plus (BMG LABTECH, Germany) at an excitation wavelength of 355 nm and an emission wavelength of 460 nm. We determined enzyme activities over a range of substrate concentrations from low to high (0 μmol g^{-1} soil, 20 μmol g^{-1} soil, 40 μmol g^{-1} soil, 60 μmol g^{-1} soil, 80 μmol g^{-1} soil, 100 μmol g^{-1} soil, 200 μmol g^{-1} soil, and 400 μmol g^{-1} soil) to ensure the appropriate saturating concentration.

Enzyme activities (V_{max}) were denoted as released MUF/AMC in nmol per g dry soil per hour (nmol MUF/AMC g^{-1} soil h^{-1}) (Awad et al., 2012), and the affinity constant for each enzyme (K_m) was expressed in μmol substrate per g dry soil (μmol g^{-1} soil). Simultaneously, MUF/AMC concentrations of 0 nM, 10 nM, 20 nM, 30 nM, 40 nM, 50 nM, 100 nM, and 200 nM were prepared to calibrate the measurement. The Michaelis-Menten equation was used to determine the parameters of the activity of the enzyme (V):

$$V = \frac{V_{max}[S]}{K_m[S]} \quad (1)$$

where V_{max} is the maximum enzyme activity (a function of enzyme concentration), S is the substrate concentration, and K_m is the substrate concentration at half-maximal enzyme activity. Both V_{max} and K_m parameters were approximated by the Michaelis–Menten equation (1) with the non-linear regression routine of SigmaPlot (v. 12.3). Catalytic efficiency was calculated as the V_{max}-to-K_m ratio (Panikov et al., 1992). The substrate turnover rate was calculated by equation (2), where T_t is the turnover time (hours) (Zhang et al., 2020).

$$T_t = \frac{K_m \times [S]}{V_{max} + [S]} \quad (2)$$

2.7. Soil DNA extraction and 16 S rRNA gene amplicon sequencing

The distinct microbial communities (bacteria and archaea) were accessed using a metabarcoding approach (16 S rRNA amplicon sequencing). Total DNA was extracted from 0.5 g of BS and RH soil samples using the FastDNA SpinKit for Soil (MP Biomedicals Fast Prep-24 5G) according to the manufacturer's instructions. This included weighing the soil into the 2 mL bead-beating tubes containing the lysis matrix. After adding 978 μL sodium phosphate buffer and 122 μL of the MT buffer provided by the kit, samples were vortexed and adjusted for bead beating using the FastPrep-24 (2 × 30 s with a 5-min rest, speed 4). Samples were kept on ice until 250 μL of PPS (protein precipitation solution) were added. Extraction was performed according to the manufacturer's protocol, and DNA was eluted in 100 μL of DES water.

The quantity and integrity of the DNA were checked by Nanodrop and on 0.8% agarose gels, respectively. The libraries from the 16 S rRNA gene amplicon using Uni341 F and Uni806 R primers and Illumina adaptors (Illumina, San Diego, USA) were performed at Novogene (UK) using Illumina MiSeq v2 (2 × 250 bp) chemistry according to the manufacturer's instructions (Illumina, San Diego, USA). Unassembled raw amplicon data were deposited in the National Center for Biotechnology Information (NCBI) Sequence Read Archive (SRA) under BioProject PRJNA942109.

2.8. Amplicon sequence analyses

The soil sample sequences were analyzed and categorized using the Divisive Amplicon Denoising Algorithm (DADA2 v.1.12.1 pipeline; Callahan et al., 2016) in R (R Core Team, 2019). The "FilterAndTrimmed" function was utilized for the quality trimming and filtering processes. Reads of less than 100 bp were discarded, and two expected errors were permitted for each read. The subsequent steps involved error inference, denoising, and chimera removal. Following quality filtering, denoising, and chimera removal, the 16 S rRNA gene amplicon depths of 48 samples produced 1,558,139 high-quality 16 S rRNA gene reads, or 32,461 per sample. The amplicon sequencing variations (ASVs) were assigned taxonomically using the SILVA database version 138 (Quast et al., 2013) and then imported into the phyloseq tool in R (McMurdie and Holmes, 2013). Unassigned ASVs at the phylum level and any remaining ASVs identified as chloroplasts, mitochondria, or eukaryotes were omitted from the studies. Amplicon sequencing yielded 46,725 unique ASVs.

2.9. Statistical analysis

General linear models (GLMs) were used to test the difference between the means of the response variables at a significance threshold of $\alpha = 0.05$. The factors in the GLM were rotational position (KW1, KW2, and KW4), soil compartment (BS, RH), and soil depth (0–30 cm, 30–60 cm, and 60–100 cm). The Shapiro–Wilk and Levene tests as well as a visual inspection of QQ plots were used to test for normality of the residual distribution and homogeneity of variance, respectively. Pairwise comparisons were made for soil chemical and enzymatic data using Bonferroni correction to identify differences between the response variables. Data transformation was performed when the assumptions of GLM failed. Yeo–Johnson (Yeo and Johnson, 2000), Box–Cox (Box and Cox, 1964), and log transformations were used. The transformation used for a certain variable is mentioned in the respective table. Correlation analysis was performed using Pearson's correlation for the response variable and for every level of the rotational position of WW (KW1, KW2, and KW4). Since the soil sampling for microbiome data was performed only for soil depths of 0–30 cm and 30–60 cm, we calculated correlation coefficients for these two depths only, excluding the 60–100 cm layer from our analysis. Where applicable, we also show the variables related to BS and RH. The abovementioned statistical analyses were performed with IBM SPSS Statistics for Windows, version 23 (IBM Corp., Armonk, N.Y., USA). Graphs were generated with the *ggplot2* package in R (v4.2.1; R Core Team 2022).

Relative abundances, alpha and beta diversities, and statistical tests were determined in R using specialized R package functions. Rarefaction analysis within the vegan R package examined the sequencing depth (Oksanen et al., 2020). The rarefaction curves tended to reach a plateau, indicating that the sequencing method supplied sufficient sequences to cover most of the sample diversity. Microbial sequences were rarefied for the lowest number of sequences identified among all samples, generating a dataset with 22,158 sequences per sample. The alpha diversity indices were computed for each rarefied sample using the

phyloseq (McMurdie and Holmes, 2013) and *microbiome* (Lahti and Shetty, 2017) R packages. Using 10,000 permutations, Kruskal–Wallis tests were employed to evaluate for statistically significant changes in alpha diversity. The microbial composition of samples was assessed after transformation to relative abundance. The differences in phyla and taxa across samples were visualized using the *phyloseq* package (McMurdie and Holmes, 2013). Permutational multivariate analysis of variance (PERMANOVA) was performed to identify significant differences in the WW microbial community composition. The beta diversity of the microbial communities was visualized by a principal coordinate analysis (PCoA) using the Bray–Curtis distance.

3. Results

3.1. Effects of rotational position, soil compartment, and soil depth on winter wheat growth

The preceding crop history had a pronounced effect on the biomass of the following WW. KW2 and KW4 plants had 43 % and 45 % reduced dry weight, respectively, compared to KW1 (Table S1; Fig. 1a). The decline in wheat dry weight was attributed to a reduction in root and stem biomass for KW2, and root, stem, and leaf biomass for KW4 when compared to KW1 (Fig. 1a). Higher shoot N concentration resulted in a lower C:N ratio for KW1 compared to KW2 and KW4 (Table S1; Fig. 1b). In all rotational positions, there was a similar C:N ratio increase within roots, stems, and leaves (Table S1).

There was a strong response of root growth traits to WW rotational position with an overall reduction in RLD of 29 % and 31 % for KW2 and KW4, respectively, mainly in the upper 30 cm of the soil (Table S2; Fig. 2a). However, even at a greater depth (60–100 cm), KW1 had the highest difference in RLD compared with KW4. At this depth, KW2 increased its RLD greater than KW4, which had the lowest values of all three rotational positions. Similarly, KW1 had the highest RTD of all rotational positions, with 58 % and 48 % higher RTD values than KW2 and KW4, respectively (Table S2; Fig. 2b). These differences were apparent in both the topsoil and the subsoil. Overall, KW1 had thicker roots with an R_{dia} of 0.28 mm compared to 0.25 mm and 0.24 mm for KW2 and KW4, respectively, a trend that was observed throughout the soil profile (Table S2, Fig. 2c). The R_{dia} of all three rotational positions increased at greater soil depth (Table S2). Finally, KW2 and KW4 increased their SRL by 28 % and 33 % compared to KW1, with significant differences along the complete soil profile (Table S2, Fig. 2d).

3.2. Effects of rotational position, soil compartment, and soil depth on biochemical soil properties

More ammonium (NH_4^+) and nitrate (NO_3^-) were found in the RH compared to BS and in the 0–30 cm soil layer compared to subsoil layers (Table S3). The rotational position of WW strongly affected mineral N, with a 42 % and 48 % lower NH_4^+ concentration in KW1 overall compared to KW2 and KW4, respectively (Fig. 3a). In particular, in the uppermost soil depth of KW1, there was much less NH_4^+ than in the same depth of KW2 (−54 %) and KW4 (−58 %). In addition, a similarly lower NO_3^- content was found in KW1 (−49 % and −36 % compared to KW2 and KW4, Fig. 3b). Microbial biomass C (C_{mic}) and N (N_{mic}) were also highly impacted by the rotational position, as shown in Fig. 4. C_{mic} was lower by 37 % and 43 % in KW1 compared to KW2 and KW4, respectively (Fig. 4a). N_{mic} values of KW1 were 50 % and 57 % lower than those of KW2 and KW4 (Fig. 4b). Most C_{mic} and N_{mic} were found in the topsoil (Table S2).

The rotational position also had a major influence on DOC levels (Table S3). KW1 soil had 68 % and 150 % higher DOC concentrations than KW2 and KW4, respectively (Fig. S2). A significant main effect of soil compartment was shown, with a 74 % higher DOC content in the RH compared to BS. Interestingly, the DOC level in the RH of KW1 at both subsoil depths (30–60 and 60–100 cm) was 1.7 and 4.1 times higher than KW2 and KW4, respectively (Fig. S2). Similar DOC concentrations were observed in the BS in the rotational position and at all three soil depths.

3.3. Effects of rotational position, soil compartment, and soil depth on extracellular enzymes activities

The maximum reaction rate (V_{max}) of BGU was higher in KW2 compared to KW4 (by 27 %). No differences were observed between BS and RH, while higher values were observed in the first 30 cm of the soil profile (Table S4). The interaction between rotational position, soil compartment, and soil depth revealed a 91 % and 169 % higher BGU V_{max} in the RH of KW1 at 30–60 cm and 60–100 cm of the subsoil, respectively, compared to KW4. In contrast, KW2 and KW4 had a higher

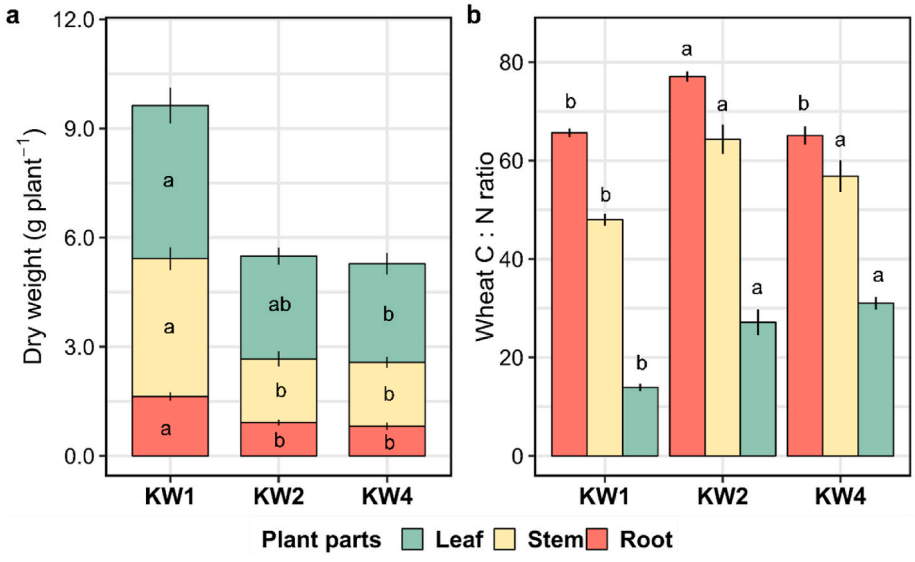

Fig. 1. Effect of the rotational positions on root, stem, leaf dry weight (a) and C:N ratio (b) of the following winter wheat at onset of stem elongation (BBCH 30). KW1 = first wheat, KW2 = second wheat, and KW4 = fourth wheat after oilseed rape in soil from the experimental farm Hohenschulen in Kiel, Germany. Within each plant part, different lowercase letters denote significant differences between rotational positions at $p \leq 0.05$ according to ANOVA with Bonferroni correction for multiple comparisons.

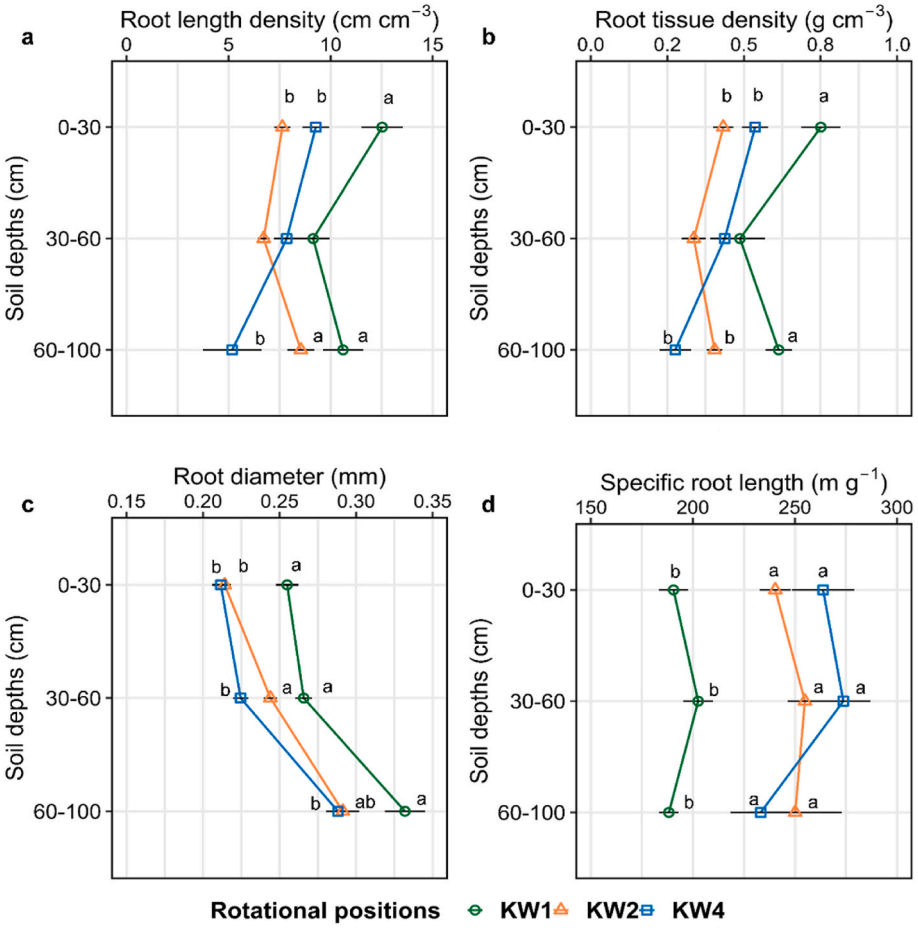

Fig. 2. Effect of the rotational positions on root length density (a), root tissue density (b), average root diameter (c) and specific root length (d) of the following winter wheat at the onset of stem elongation (BBCH 30) at soil depths 0–30 cm, 30–60 cm and 60–100 cm). KW1 = first wheat, KW2 = second wheat, and KW4 = fourth wheat after oilseed rape in soil from the experimental farm Hohenschulen in Kiel, Germany. Within each soil depth, different lowercase letters denote significant differences between rotational positions at $p \leq 0.05$ according to ANOVA with Bonferroni correction for multiple comparisons. No letters indicate non-significant differences.

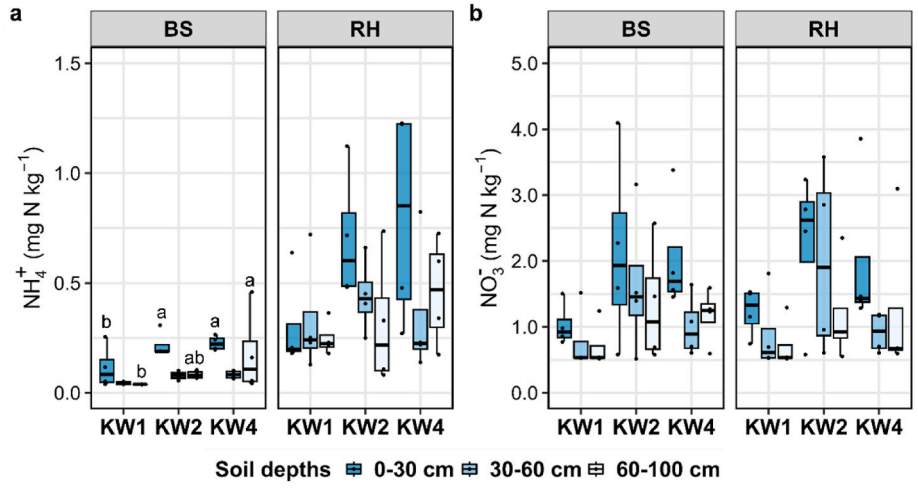

Fig. 3. Effect of the rotational positions on soil NH_4^+-N (a) and NO_3^--N (b) of the following winter wheat at onset of stem elongation (BBCH 30) at soil depths 0–30 cm, 30–60 cm and 60–100 cm and two soil compartments bulk soil (BS) and rhizosphere soil (RH). KW1 = first wheat, KW2 = second wheat, and KW4 = fourth wheat after oilseed rape in soil from the experimental farm Hohenschulen in Kiel, Germany. Within each soil depth and soil compartment, different lowercase letters denote significant differences between rotational positions at $p \leq 0.05$ according to ANOVA with Bonferroni correction for multiple comparisons. No letters indicate non-significant differences.

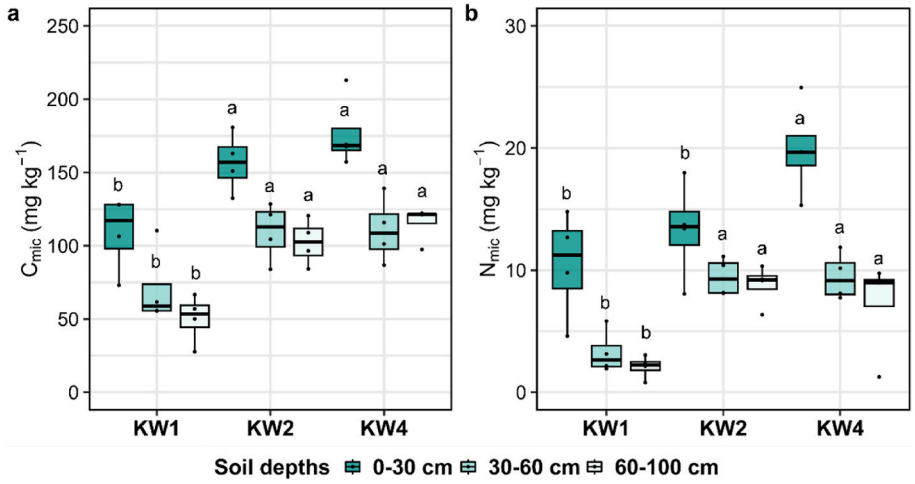

Fig. 4. Effect of the rotational positions on microbial biomass carbon (C_{mic}, a) and microbial biomass nitrogen (N_{mic}, b) of the following winter wheat at onset of stem elongation (BBCH 30) at soil depths 0–30 cm, 30–60 cm and 60–100 cm. KW1 = first wheat, KW2 = second wheat, and KW4 = fourth wheat after oilseed rape in soil from the experimental farm Hohenschulen in Kiel, Germany. Within each soil depth, different lowercase letters denote significant differences between rotational positions at $p \leq 0.05$ according to ANOVA with Bonferroni correction for multiple comparisons. No letters indicate non-significant differences.

BGU V_{max} in the topsoil compared to KW1 (by 83 % and 89 %, respectively; Fig. S5a). The response of the BGU substrate affinity (K_m) to the rotational position revealed a 64 % and 68 % reduction in affinity for KW2 and KW4 compared to KW1, which was evident in all soil layers (Fig. S5b). A higher catalytic efficiency (K_a) was observed in KW1 compared to KW2 and KW4, while a lower substrate turnover time (Tt) was seen in KW1 and KW2 compared to KW4 (Table S4). The V_{max} of the leucine aminopeptidase (LAP) of KW1 equaled that of KW2 and was 32 % higher than that of KW4 (Fig. S5c). It was also increased in BS compared to RH, with no obvious differences in its response between soil depths. Higher values of V_{max} were observed in the BS of KW1 in the subsoil layers compared to KW2 and KW4. Soil compartment had a significant effect, with LAP affinity increasing in the RH compared to BS (Table S4). LAP K_m was also affected by the rotational position, as shown in Fig. S5d. KW2 had a much higher LAP affinity in the RH than BS, while it did not fluctuate significantly between the two soil compartments for KW1 and KW4. LAP K_m was higher in KW1 compared to KW4 in the BS (58 %) and RH (76 %) (Fig. S5d). Finally, both K_a and Tt were increased in KW4 compared to KW1 and KW2 (Table S4).

Zymography revealed significant differences between WW rotations (Table S5), with the BGU rhizosphere extent of KW1 averaging 5.3 mm compared with 2.5 mm for KW2 and KW4. This response was mainly driven by major differences in the lowest soil depth, where the rhizosphere extent for BGU was 9 mm compared to 4 mm for KW2 and 3 mm for KW4 (Fig. 5a). In a similar manner, the rhizosphere extent for LAP was, on average, 0.36 mm for KW1, which was significantly higher than for KW4 (0.16 mm, Fig. 5b). We found a similar, though insignificant, trend of a reduced LAP rhizosphere extent for KW2 (0.19 mm). In terms of BGU and LAP activity, there were no pronounced differences among the fixed factors of the experiment (Fig. 5c and d). The same was true for the BGU hotspot area, with a decreasing hotspot area percentage at greater soil depths that was nonetheless insignificant (Fig. 5e). Lastly, the LAP hotspot area for KW1 was 96 % higher than KW2 in the deep subsoil of 60–100 cm (Fig. 5f).

Glucose (GLU) imaging revealed significant differences between the GLU rhizosphere extent and hotspot area between the three soil layers (Table S5). This trend followed that of the root growth data. We also observed a decreasing rhizosphere extent for GLU in successively grown WW that was, however, insignificant (Fig. 6a). The same was found for GLU release per surface area (Fig. 6b), with a lower relative amount of GLU release in KW2 and KW4, although there was no significant main effect of the rotational position. However, a significant decline was recorded in the GLU hotspot area in the 60–100 cm layer of the soil profile in KW2 (−53 %) compared to KW1 (Fig. 6c).

3.4. Effects of rotational position, soil compartment, and soil depth on microbial community structure and composition

A significant difference in species richness between KW1 and KW4 was observed in the BS compartment and in the uppermost 30 cm of soil, where KW4 presented a higher number of species than KW1 (Fig. S6a). Interestingly, there was no influence on the microbial community diversity and species evenness distribution expressed as the Pielou index and Shannon index, respectively (Figs. S7a and b). The soil depth had a main effect on the beta diversity parameters (Fig. S6b). According to the PERMANOVA results, the rotational position explained 10.5 % of the variation ($F = 3.51$; $p < 0.001$) in the microbial community, while soil depth explained 12.3 % of the variation observed ($F = 5.97$; $p < 0.001$).

The main components of the microbial community composition at the phylum level were *Actinobacteriota*, *Proteobacteria*, *Chloroflexi*, *Gemmatimonadota*, and *Crenarchaeota*. The relative abundance of several taxa from *Acidobacteriota*, *Gemmatimonadota*, *Nitrospirota*, and *Chloroflexi* was significantly affected by the rotational position in the BS and RH soils and at different soil depths. While in the BS of the plants, the relative abundance of *Acidobacteriota* was not significantly different, we recorded a significantly higher relative abundance of *Acidobacteriota* in the RH of the topsoil and subsoil of KW1 compared to both KW2 and KW4 (Fig. 7a). A decreasing relative abundance of *Gemmatimonadota* in KW4 compared to KW1 was found in both soil compartments, while the difference between KW1 and KW2 remained insignificant (Fig. 7b). With regard to *Nitrospirota*, KW1 and KW2 had similar relative abundances in both BS and the RH (Fig. 7c). In the RH, the relative abundance of *Nitrospirota* was significantly higher in both the topsoil and subsoil of KW2 compared to KW4. Finally, in KW1 and KW2, there was a much lower relative abundance of *Chloroflexi* compared to KW4, and this difference was consistently found in BS and RH soil (Fig. 7d).

In order to examine the relationship between the measured parameters in each rotational position and their influence on the different bacterial phyla, we conducted correlation analyses (Tables S9–S11). At 0–30 cm, the root dry weight of KW1 was negatively correlated with the relative abundance of *Gemmatimonadota* in the rhizosphere compartment. At 30–60 cm, it was positively correlated with the soil NO_3^- content in the BS, K_{CAL} in the RH, and the relative abundance of *Nitrospirota* in the RH, but negatively correlated with *Chloroflexi* in the RH and *Acidobacteriota* in the BS (Table S9). For KW4, the root dry weight was negatively correlated with the relative abundance of *Chloroflexi* in the

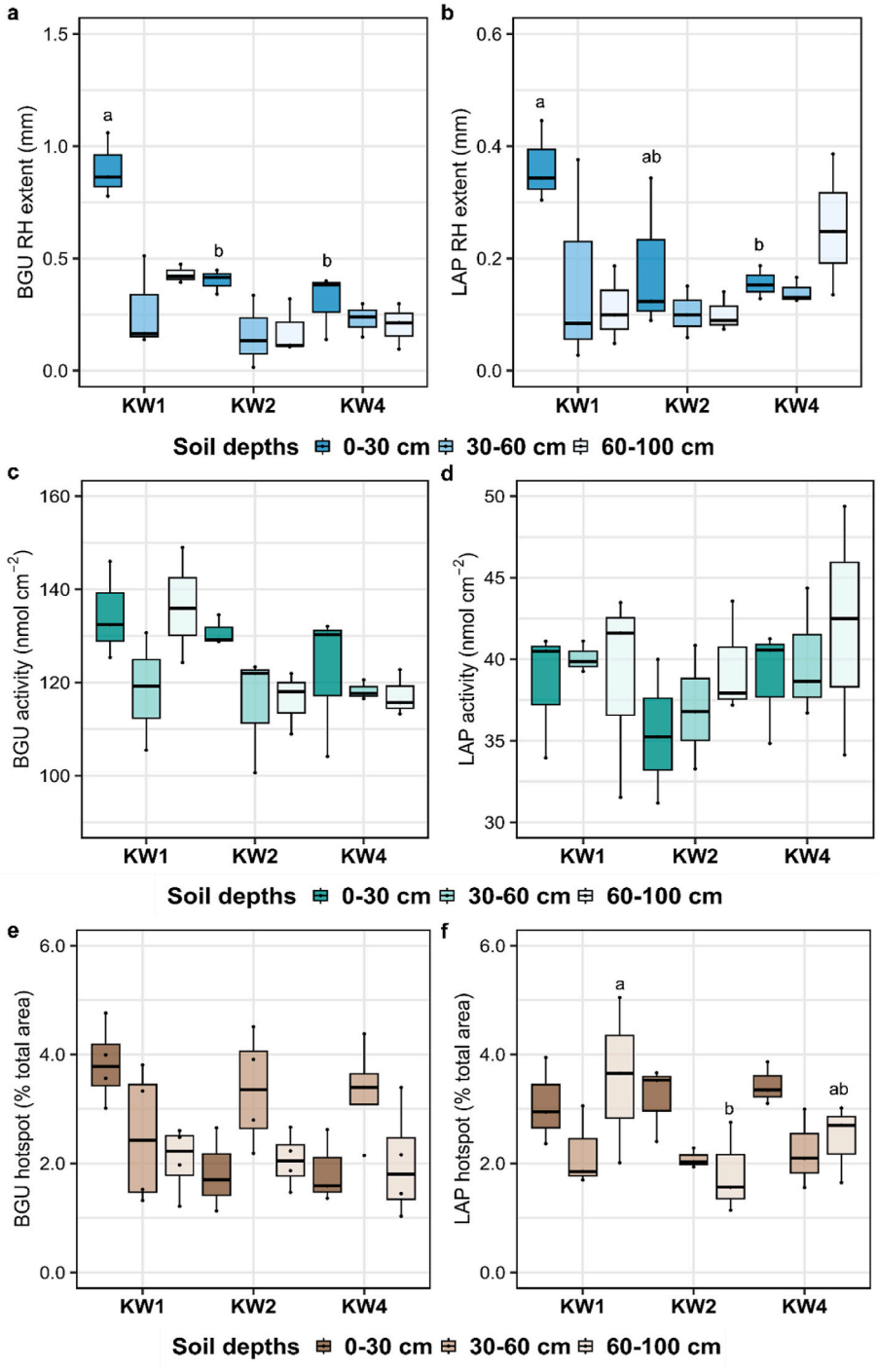

Fig. 5. Effect of the rotational positions on rhizosphere extent (RH), activity and hotspot percentage of β-glucosidase (BGU) (a, c, e) and leucine aminopeptidase (LAP) (b, d, f) of the following winter wheat at onset of stem elongation (BBCH 30) at soil depths 0–30 cm, 30–60 cm and 60–100 cm. KW1 = first wheat, KW2 = second wheat, and KW4 = fourth wheat after oilseed rape in soil from the experimental farm Hohenschulen in Kiel, Germany. Within each soil depth and soil compartment, different lowercase letters denote significant differences between rotational positions at $p \leq 0.05$ according to ANOVA with Bonferroni correction for multiple comparisons. No letters indicate non-significant differences.

RH and *Nitrospirota* in the RH (Table S11). For KW1 and at 30–60 cm, DOC was positively correlated with P_{CAL} in the RH. DOC was also positively correlated with both the BGU and LAP reaction rates in the BS. Finally, DOC positively correlated with the relative abundance of *Nitrospirota* in the RH (Table S9). For KW2 and at 0–30 cm, DOC was negatively correlated with K_{CAL} in the BS. In the RH, there was a negative correlation between DOC and C_{mic} and a positive correlation between DOC and the relative abundance of *Acidobacteriota*. As for KW4, there was a negative correlation between DOC in the RH and BGU rhizosphere extent (Table S11). C_{mic} exhibited a positive correlation with the LAP hotspot at 0–30 cm of KW1, while it was negatively correlated with *Gemmatimonadota* in the BS. At 30–60 cm, it was positively correlated with both NO_3^- of the RH and N_{mic} (Table S9). C_{mic} of KW2 was negatively correlated with both *Chloroflexi* and *Acidobacteriota* in the RH at 0–30 cm. In the subsoil, it was negatively correlated with DOC in the RH (Table S10). Finally, in the topsoil of KW4, C_{mic} was positively correlated with both NH_4^+ and NO_3^- in the RH and BS, respectively (Table S11).

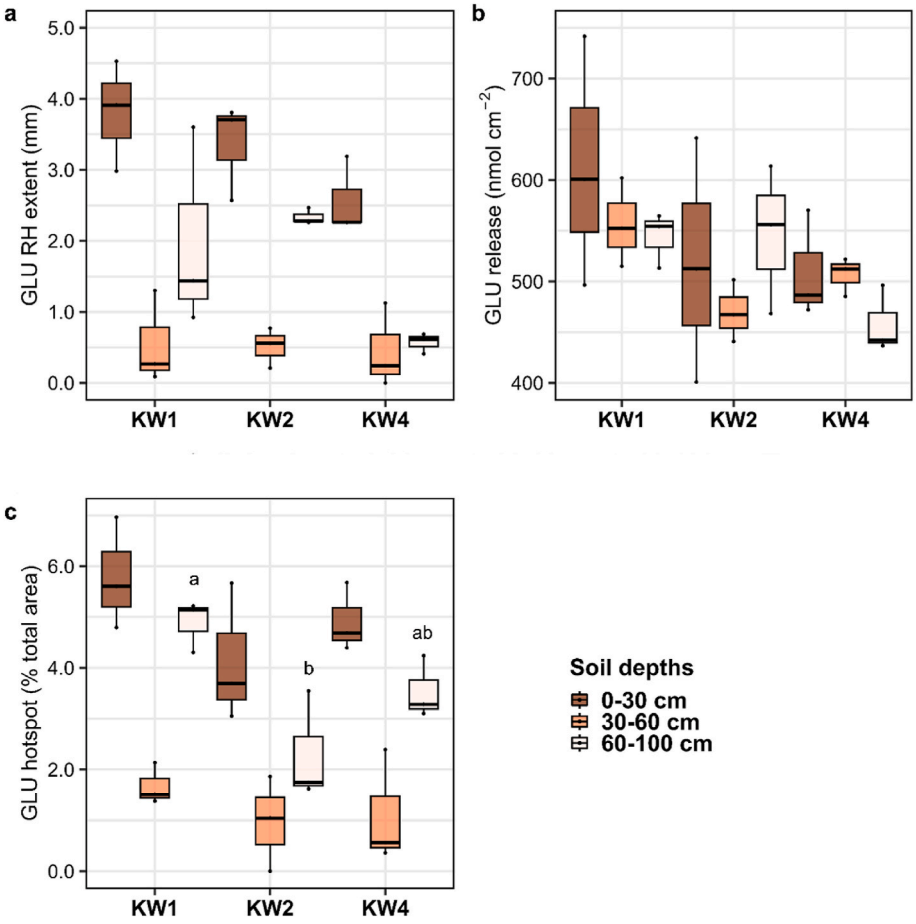

Fig. 6. Effect of the rotational positions on glucose rhizosphere extent (RH, a), release (b) and hotspot percentage (c) of the following winter wheat at onset of stem elongation (BBCH 30) at soil depths 0–30 cm, 30–60 cm and 60–100 cm. KW1 = first wheat, KW2 = second wheat, and KW4 = fourth wheat after oilseed rape in soil from the experimental farm Hohenschulen in Kiel, Germany. Within each soil depth and soil compartment, different lowercase letters denote significant differences between rotational positions at $p \leq 0.05$ according to ANOVA with Bonferroni correction for multiple comparisons. No letters indicate non-significant differences.

4. Discussion

4.1. Root plastic responses drive nutrient supply and plant biomass accumulation in winter wheat rotations

Successively grown WW appeared to prioritize soil exploration, shaping a thinner and less dense root system, as indicated by its higher SRL, lower R_{dia}, and RTD. It should be noted that the overall RLD and SRL followed a similar trend for each measured diameter class in the rotational positions. In a field trial with silty loam soil, Arnhold et al. (2023b) found no differences in RLD between the first WW after oilseed rape, the second WW after oilseed rape, and WW monoculture at the end of tillering. However, when they measured RLD during late flowering in a year with high summer precipitation, the wheat after oilseed rape had a significantly higher RLD than the successively grown WW in the topsoil. In the sandy loam soil of our study, we documented an early reduction in RLD in successive WW rotations during the relatively dry period of the trial (Fig. S1). Therefore, the soil type and environmental conditions are strong determinants of the effect of the WW rotational position on its plant biomass accumulation.

Differences in root growth patterns might explain the more efficient N, P, and K uptake in KW1, leading to lower mineral N, P, and K concentrations in the soil of KW1 at BBCH 30 and, therefore, an increased N, P, and K supply to the plants, which is reflected in the lower C:N ratios of KW1 compared to KW2 and KW4 (Fig. 1a and b; Table S6). A higher N uptake by maize plants was previously found in diversified crop rotations (maize, soybean, three-year wheat rotation with red clover and rye cover crops) and was associated with a higher C and N enzymatic activity of soil microbes (Bowles et al., 2022). In our study, there was a positive correlation between the root dry weight and the K_{CAL} in the topsoil of KW1, but this was not the case for KW2 and KW4. In the topsoil, the SRL of KW1 was negatively correlated with NH_4^+ in the RH and K_{CAL} (Table S9). The SRL of plants tends to increase under biotic and abiotic stresses (Kramer-Walter et al., 2016; Kaloterakis et al., 2021; Spitzer et al., 2021), while RLD and R_{dia} are reduced (Kramer-Walter et al., 2016; Lopez et al., 2023). Accordingly, the SRL of KW2 was negatively correlated with RLD and the root dry weight (Table S10). Kelly et al. (2022) found a higher SRL in WW landraces grown under conditions of low nutrient availability, while landraces with a higher proportion of coarse roots were associated with higher extractable C pools in the RH. The higher NH_4^+ was positively correlated with the R_{dia} of KW1, especially in the subsoil (Table S9). KW1 is also associated with high residual mineral N in the soil after harvest (10–20 kg N ha^{-1}) that is readily available for uptake by KW1 (Weiser et al., 2018). Our data suggest that this available N stimulated the early growth of KW1, enabling the vigorous establishment and exploitation of the rhizobox soil volume. Due to their initial root growth reduction, KW2 and KW4 did not fully utilize the N reservoir of the soil, resulting in higher mineral N in the soil at the end of the experiment.

4.2. High microbial biomass and low labile carbon in the soil of successive winter wheat rotations induce nitrogen immobilization

In a recent field experiment, Yang et al. (2022) found that C_{mic} and

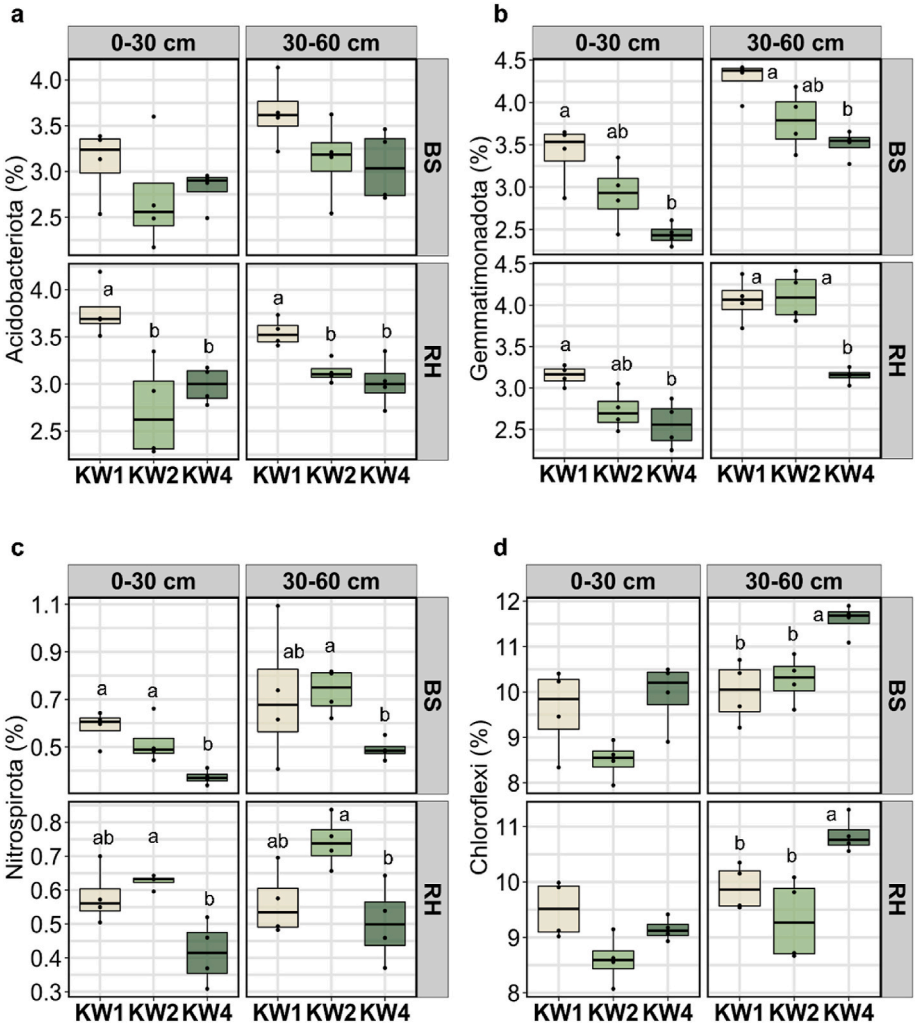

Fig. 7. Effect of the rotational positions on the relative abundance of (a) *Acidobacteriota*, (b) *Gemmatimonadota*, (c) *Nitrospirota* and (d) *Chloroflexi* at soil depths 0–30 cm and 30–60 cm, in the two soil compartments bulk soil (BS) and rhizosphere (RH). KW1 = first wheat, KW2 = second wheat, and KW4 = fourth wheat after oilseed rape in field soil from the experimental farm Hohenschulen in Kiel, Germany. Within each soil depth and soil compartment, different lowercase letters denote significant differences between rotational positions at $p \leq 0.05$ according to ANOVA with Bonferroni correction for multiple comparisons. No letters indicate non-significant differences.

N_{mic} increased in parallel with WW dry matter accumulation throughout the growth period. In our experiment, the highest plant biomass-yielding rotational position, KW1, had much lower C_{mic} and N_{mic} values at all three soil depths, confirming the results of the aforementioned study. Typically, higher root biomass is associated with increased microbial biomass (Lange et al., 2015). However, changes in root biomass may be more accurately linked to changes in microbial diversity, thus explaining the trends observed (Fig. S6) in this experiment (Ren et al., 2017). Hansen et al. (2019) reported a similar decline in C_{mic} when oilseed rape was introduced into successive wheat monocultures and attributed this effect to the biocidal properties of its secondary metabolite, isothiocyanate. The initial soil biochemical properties of the three rotational positions (Table 1) showed a higher C_{mic} in the soil of KW4 and a higher C_{mic}:N_{mic} ratio for KW2 compared to KW1. The higher C_{mic}, C_{mic}:N_{mic} ratio, and lower soil mineral N indicate a significant initial N limitation of the soil microbial community of successively grown WW. The high initial DOC content of the soil (Table 1) induced rapid microbial regrowth after the initial adjustment of the water-holding capacity (WHC), resulting in N immobilization that may have affected plant growth. The higher C_{mic} measured at the end of the experiment was not utilized as an N source (i.e. mineralization of microbial biomass and N release) by KW2 and KW4, leading to lower plant biomass and a higher plant C:N ratio.

4.3. Microbial activity in the rhizosphere of winter wheat is highly dependent on its rotational position

The combination of zymography with the quantification of enzyme kinetic parameters complemented each other and improved our understanding of the microbial activity and the nutrient transformations in the RH of WW. Zymography is an invaluable technique to demonstrate the dynamics of enzymatic activity at very small spatial scales (Razavi et al., 2019; Guber et al., 2021). Soil microbes in successive WW rotations invested less in BGU and LAP secretion compared to those in the RH of KW1, especially in the subsoil. The absence of the main effect of soil depth on soil enzymatic activity, together with the high root growth and DOC content in the subsoil, imply that the soil microbes sustained their metabolic function at greater depth. This was evident for all three rotational positions.

The zymograms of BGU and LAP showed a narrower rhizosphere extent in the topsoil of KW2 and KW4 compared to KW1 (Fig. 5). This suggests that the root system of KW1 stimulated microbial activity, increasing glucose and leucine release, which can be directly utilized by microbes. As a result, the microbes in the RH of KW1 (and partially of

KW2) (such as taxa belonging to the *Gemmatimonadota*, *Acidobacteriota*, and *Nitrospirota*) were able to utilize the DOC and N in the RH more effectively than the microbes in the RH of KW4 (Fig. 3, Fig. S2). Plants as well as bacteria and archaea (Singh et al., 2016; Bilyera et al., 2021) produce BGU, an enzyme important in the first step of cellulose degradation, which is the major component of plant cell walls. Microbes have a weaker ability to utilize low molecular weight C when competing with plants for available nutrients, with DOC content being a strong determinant of the outcome of this interaction (Kuzyakov and Jones, 2006; Song et al., 2020). Complementing our findings on the DOC of the RH, we found a larger glucose hotspot area in KW1 compared to KW2 and KW4. Labile C is considered critical for maintaining the pathogen-suppressive qualities of agricultural soils, irrespective of the total soil organic matter content (Bongiorno et al., 2019), which could have confounded the biocidal soil legacy of oilseed rape.

Depth-specific comparisons revealed differences in the activity of the previous C- and N-cycling soil enzymes between all three rotational positions. Interestingly, BGU activity was significantly higher in the RH and in the topsoil of KW2 and KW4 than in KW1. This pattern could be explained by the accumulation of less labile organic matter from the wheat residues in the uppermost soil layers in successively grown WW (Cenini et al., 2016; Ni et al., 2020; Luan et al., 2022), which may have stimulated the growth of cellulose-degrading microbes. This, in turn, led to higher BGU activity in the topsoil and C_{mic} throughout the soil profile (Zhao and Zhang, 2018; Reichel et al., 2022). Soil microorganisms thus synthesize BGU in response to the presence of a decomposable substrate that must be degraded (Turner et al., 2002; Veres et al., 2015).

The larger LAP hotspot area in KW1 compared to successively grown WW indicates a larger overall rhizosphere size, which affects a larger soil volume and thus induces positive soil feedback for KW1. This may have contributed to the observed N limitation of successively grown WW. Protein-derived N accounts for 40 % of total soil N and is a crucial N source for microbes and plants, but it is also a precursor for mineral N production that is available for plant uptake (Rillig et al., 2007; Paungfoo-Lonhienne et al., 2008; Näsholm et al., 2009). It is likely that these differences in the form of organic N in the soil of the rotational position stimulated LAP activity in KW1 and repressed it in successively grown WW, with an increasing size of effect from KW2 to KW4. Emmett et al. (2020) showed that plant N uptake and LAP activity are coupled in sunflower (*Helianthus annuus* L.), buckwheat (*Fagopyrum esculentum* Moench), Sudan grass (*Sorghum* x *drummondii* (Nees ex Steud.) Millsp. & Chase), Japanese millet (*Echinochloa esculenta* (A. Braun) H. Scholz), and maize (*Zea mays* subsp. *mays* L.) during flowering, and attributed this to the priming of soil organic N that is available for plant uptake. We observed that higher concentrations of DOC and NH_4^+ were accompanied by higher LAP activity and substrate affinity in the RH (Fig. S5, Fig. 5). However, the literature is inconclusive regarding the impact of inorganic N on LAP activity (Cenini et al., 2016; Shi et al., 2016).

4.4. The rotational position of WW shapes the soil microbial community composition

The higher richness of bacterial taxa in the BS of KW4 compared to KW1 and KW2 suggests that successive wheat cultivation selects a broader spectrum of bacteria that are better adapted to the specific soil conditions (Mayer et al., 2019). Previous research has shown that preceding crops affect the microbial communities in the wheat rhizosphere (Hilton et al., 2018; Babin et al., 2019). Oilseed rape is known to recruit microbial taxa that enhance the growth of the following WW (Vujanovic et al., 2012). This might be linked to the control that the preceding crops exert over the quantity and quality of the secreted exudates, leading to changes in the relative abundance of certain taxa (Jones et al., 2019; Wen et al., 2022). In addition, we observed only minor differences between BS and RH soil compartments, which is in contrast to other studies reporting pronounced differences between soil- and root-associated communities (Schreiter et al., 2014; Bziuk et al., 2021). These findings suggest that our non-destructive sampling technique using microspatulas may have been constrained by the distance at which we were able to collect soil samples from the vicinity of the plant roots (≤5 mm). Although more precise techniques, such as the wet needle technique (Tian et al., 2020) or Stomacher blending to wash off tightly adhering soil particles directly from the roots, could provide a better distinction between BS and RH microbial communities, they are mainly suitable for only very small sample sizes in terms of soil weight, or they require more root material. Nevertheless, we aimed for a compromise in sampling RH and BS to be able to link all gathered data, i.e. soil biochemical, enzymatic, and microbial community data.

We observed shifts in the bacterial composition at the phylum level between different WW rotational positions (Fig. 7) that might explain a potential imbalance or dysbiosis effect in successively grown WW, leading to less efficient nutrient uptake and lower plant biomass yields. In general, the microbial community structures of KW1 and KW2 were more similar compared to KW4 (Fig. S6b). It appears that the higher rate of WW residue return in the soil of WW monocropping may have favored a higher species richness, resulting in microbial taxa competing for slowly degradable C sources (straw) but causing less efficient plant nutrient supply and thus an early reduction of plant growth.

In more detail, we observed a higher relative abundance of *Acidobacteriota* in the RH of KW1 throughout the soil profile compared to KW2 and KW4. *Acidobacteriota* is considered a keystone phylum in the RH of wheat (Kavamura et al., 2020). Bacteria belonging to this phylum have been found to induce auxin (IAA) production in *Arabidopsis*, increase iron uptake following siderophore synthesis, and secrete exopolysaccharides, forming biofilms (Kielak et al., 2016; Kaloterakis et al., 2021). In the subsoil of KW2, the high microbial biomass was negatively associated with the relative abundance of *Acidobacteriota* (Tables S9–S10), which was not the case for KW1, thus highlighting the rotational position-specific effect on supporting the proliferation of certain bacterial phyla. *Chloroflexi* and *Nitrospirota* are considered to be NO_2^- oxidizers, contributing to nitrification and, therefore, soil NO_3^- production (Pivato et al., 2021; Yuan et al., 2023). *Nitrospirota* was more prevalent in KW1 and KW2 compared to KW4 in the RH. In the topsoil of KW1, we found that *Nitrospirota* was negatively associated with *Chloroflexi* in the RH (Table S9), indicating a competition for the same resources. In a rape–rice rotation, Yuan et al. (2023) correlated the relative abundance of *Nitrospirota* to urease activity, which generates NH_4^+ and, therefore, allows N turnover due to nitrification. We found that KW1 formed a more extensive root system and accumulated more N in its biomass. It could thus exploit the newly produced NH_4^+ and NO_3^- more effectively than KW2 and KW4, leading to an increase in biomass in KW1. These findings suggest functional differences in the bacterial communities of the rotational positions, underscoring the dynamic biochemical soil processes that lowered the performance of successively grown wheat.

Understanding the shape of the fungal communities of the rotational positions would help us to better comprehend the complex plant–microbe interactions. Woo et al. (2022) found a strong effect of the rotational position of wheat grown after pea on shaping bacterial and fungal diversity. In another study, fungal community composition responded more than bacterial composition to crop rotation, with a higher relative abundance of beneficial microbes in rotation canola compared to oilseed rape monocropping (Town et al., 2023). Finally, differences in the stability of bacterial and fungal necromass (reflected in the stability between peptides and chitin/chitosan) could determine the mineralization rate of immobilized N by microorganisms and, therefore, the subsequent mineral N release (Camenzind et al., 2023) that is available for uptake by WW.

5. Conclusions

In this study, three rotational positions of WW were contrasted to assess their impact on soil microbial dynamics, extracellular enzymatic

activity, and the performance of WW. We linked the activities of C-acquiring (BGU) and N-acquiring (LAP) enzymes to changes in biochemical soil processes and microbiome community in the RH of successive WW rotations. The reduced root growth and labile C in the RH of successive WW rotations led to decreased microbial and enzymatic activity and, finally, plant nutrient uptake and biomass accumulation. Our results greatly increase our understanding of the preceding crop's soil legacy, which drives the reduction in biomass growth during the early growth of WW.

Funding

This work was funded by the German Federal Ministry of Education and Research (BMBF) in the framework of the funding initiative "Rhizo4Bio - Importance of the Rhizosphere for the Bioeconomy", project "RhizoWheat" (grant number 031B0910B).

CRediT authorship contribution statement

Nikolaos Kaloterakis: Writing – review & editing, Writing – original draft, Visualization, Validation, Software, Methodology, Investigation, Formal analysis, Data curation, Conceptualization. **Mehdi Rashtbari:** Writing – review & editing, Visualization, Methodology, Data curation. **Bahar S. Razavi:** Writing – review & editing, Project administration, Methodology. **Andrea Braun-Kiewnick:** Writing – review & editing, Visualization, Methodology. **Adriana Giongo:** Writing – review & editing, Visualization, Software, Methodology, Data curation. **Kornelia Smalla:** Writing – review & editing, Project administration, Methodology. **Charlotte Kummer:** Methodology. **Sirgit Kummer:** Methodology. **Rüdiger Reichel:** Writing – review & editing, Methodology. **Nicolas Brüggemann:** Writing – review & editing, Supervision, Resources, Project administration, Investigation, Funding acquisition, Conceptualization.

Declaration of competing interest

The authors declare that they have no known competing financial interests or personal relationships that could have appeared to influence the work reported in this paper.

Data availability

The data have been uploaded to the BonaRes Repository for Soil and Agricultural Research Data; https://doi.org/10.20387/bonares-67q1-90wr. Raw amplicon data were deposited in the National Center for Biotechnology Information (NCBI) Sequence Read Archive (SRA) under BioProject PRJNA942109.

Acknowledgements

The authors acknowledge Henning Kage, Nora Honsdorf and Katharina Pronkow (at the Christian-Albrechts-University of Kiel, CAU) for providing the soil and seed material for the experiment, as well as the technical support of Holger Wissel in the soil and plant C and N analyses.

Appendix A. Supplementary data

Supplementary data to this article can be found online at https://doi.org/10.1016/j.soilbio.2024.109343.

References

Angus, J.F., Kirkegaard, J.A., Hunt, J.R., Ryan, M.H., Ohlander, L., Peoples, M.B., 2015. Break crops and rotations for wheat. Crop & Pasture Science 66, 523–552. https://doi.org/10.1071/CP14252.

Arnhold, J., Grunwald, D., Braun-Kiewnick, A., Koch, H.-J., 2023a. Effect of crop rotational position and nitrogen supply on root development and yield formation of winter wheat. Frontiers of Plant Science 14. https://doi.org/10.3389/fpls.2023.1265994.

Arnhold, J., Grunwald, D., Kage, H., Koch, H.J., 2023b. No differences in soil structure under winter wheat grown in different crop rotational positions. Canadian Journal of Soil Science 00, 1–8. https://doi.org/10.1139/cjss-2023-0030.

Awad, Y.M., Blagodatskaya, E., Ok, Y.S., Kuzyakov, Y., 2012. Effects of polyacrylamide, biopolymer, and biochar on decomposition of soil organic matter and plant residues as determined by ^{14}C and enzyme activities. European Journal of Soil Biology 48, 1–10. https://doi.org/10.1016/j.ejsobi.2011.09.005.

Babin, D., Deubel, A., Jacquiod, S., Sørensen, S.J., Geistlinger, J., Grosch, R., Smalla, K., 2019. Impact of long-term agricultural management practices on soil prokaryotic communities. Soil Biology and Biochemistry 129, 17–28. https://doi.org/10.1016/j.soilbio.2018.11.002.

Bennett, J.A., Klironomos, J., 2019. Mechanisms of plant–soil feedback: interactions among biotic and abiotic drivers. New Phytologist 222, 91–96. https://doi.org/10.1111/nph.15603.

Bilyera, N., Zhang, X., Duddek, P., Fan, L., Banfield, C.C., Schlüter, S., Carminati, A., Kaestner, A., Ahmed, M.A., Kuzyakov, Y., Dippold, M.A., Spielvogel, S., Razavi, B.S., 2021. Maize genotype-specific exudation strategies: an adaptive mechanism to increase microbial activity in the rhizosphere. Soil Biology and Biochemistry 162, 108426. https://doi.org/10.1016/J.SOILBIO.2021.108426.

Bongiorno, G., Postma, J., Bünemann, E.K., Brussaard, L., de Goede, R.G.M., Mäder, P., Tamm, L., Thuerig, B., 2019. Soil suppressiveness to *Pythium ultimum* in ten European long-term field experiments and its relation with soil parameters. Soil Biology and Biochemistry 133, 174–187. https://doi.org/10.1016/j.soilbio.2019.03.012.

Bowles, T.M., Jilling, A., Morán-Rivera, K., Schnecker, J., Grandy, A.S., 2022. Crop rotational complexity affects plant-soil nitrogen cycling during water deficit. Soil Biology and Biochemistry 166, 108552. https://doi.org/10.1016/j.soilbio.2022.108552.

Box, G.E.P., Cox, D.R., 1964. An analysis of transformations. Journal of the Royal Statistical Society: Series B 26, 211–243. https://doi.org/10.1111/J.2517-6161.1964.TB00553.X.

Bziuk, N., Maccario, L., Douchkov, D., Lueck, S., Babin, D., Sørensen, S.J., Schikora, A., Smalla, K., 2021. Tillage shapes the soil and rhizosphere microbiome of barley—but not its susceptibility towards Blumeria graminis f. sp. hordei. FEMS Microbiology Ecology 97, fiab018. https://doi.org/10.1093/femsec/fiab018.

Callahan, B.J., Mcmurdie, P.J., Rosen, M.J., Han, A.W., Johnson, A.J.A., Holmes, S.P., 2016. DADA2: high-resolution sample inference from Illumina amplicon data. Nature Methods 13, 581–583. https://doi.org/10.1038/nmeth.3869.

Camenzind, T., Mason-Jones, K., Mansour, I., Rillig, M.C., Lehmann, J., 2023. Formation of necromass-derived soil organic carbon determined by microbial death pathways. Nature Geoscience 16, 115–122. https://doi.org/10.1038/s41561-022-01100-3.

Canarini, A., Kaiser, C., Merchant, A., Richter, A., Wanek, W., 2019. Root exudation of primary metabolites: mechanisms and their roles in plant responses to environmental stimuli. Frontiers in Plant Science 10, 157. https://doi.org/10.3389/fpls.2019.00157.

Cenini, V.L., Fornara, D.A., McMullan, G., Ternan, N., Carolan, R., Crawley, M.J., Clément, J.C., Lavorel, S., 2016. Linkages between extracellular enzyme activities and the carbon and nitrogen content of grassland soils. Soil Biology and Biochemistry 96, 198–206. https://doi.org/10.1016/j.soilbio.2016.02.015.

Cook, R.J., 2003. Take-all of wheat. Physiological and Molecular Plant Pathology 62, 73–86. https://doi.org/10.1016/S0885-5765(03)00042-0.

Cortois, R., Schröder-Georgi, T., Weigelt, A., van der Putten, W.H., De Deyn, G.B., 2016. Plant–soil feedbacks: role of plant functional group and plant traits. Journal of Ecology 104, 1608–1617. https://doi.org/10.1111/1365-2745.12643.

Costa, O.Y.A., Raaijmakers, J.M., Kuramae, E.E., 2018. Microbial extracellular polymeric substances: ecological function and impact on soil aggregation. Frontiers in Microbiology 9, 1–14. https://doi.org/10.3389/fmicb.2018.01636.

Dorodnikov, M., Blagodatskaya, E., Blagodatsky, S., Marhan, S., Fangmeier, A., Kuzyakov, Y., 2009. Stimulation of microbial extracellular enzyme activities by elevated CO2 depends on soil aggregate size. Global Change Biology 15, 1603–1614. https://doi.org/10.1111/J.1365-2486.2009.01844.X.

Emmett, B.D., Buckley, D.H., Drinkwater, L.E., 2020. Plant growth rate and nitrogen uptake shape rhizosphere bacterial community composition and activity in an agricultural field. New Phytologist 225, 960–973. https://doi.org/10.1111/nph.16171.

Galloway, A.F., Knox, P., Krause, K., 2020. Sticky mucilages and exudates of plants: putative microenvironmental design elements with biotechnological value. New Phytologist 225, 1461–1469. https://doi.org/10.1111/nph.16144.

German, D.P., Chacon, S.S., Allison, S.D., 2011. Substrate concentration and enzyme allocation can affect rates of microbial decomposition. Ecology 92, 1471–1480. https://doi.org/10.1890/10-2028.1.

Guber, A., Blagodatskaya, E., Juyal, A., Razavi, B.S., Kuzyakov, Y., Kravchenko, A., 2021. Time-lapse approach to correct deficiencies of 2D soil zymography. Soil Biology and Biochemistry 157, 108225. https://doi.org/10.1016/j.soilbio.2021.108225.

Hansen, J.C., Schillinger, W.F., Sullivan, T.S., Paulitz, T.C., 2019. Soil microbial biomass and fungi reduced with canola introduced into long-term monoculture wheat rotations. Frontiers in Microbiology 10, 1488. https://doi.org/10.3389/fmicb.2019.01488.

Hernández-Calderón, E., Aviles-Garcia, M.E., Castulo-Rubio, D.Y., Macías-Rodríguez, L., Ramírez, V.M., Santoyo, G., López-Bucio, J., Valencia-Cantero, E., 2018. Volatile compounds from beneficial or pathogenic bacteria differentially regulate root exudation, transcription of iron transporters, and defense signaling pathways in Sorghum bicolor. Plant Molecular Biology 96, 291–304. https://doi.org/10.1007/s11103-017-0694-5.

Hilton, S., Bennett, A.J., Chandler, D., Mills, P., Bending, G.D., 2018. Preceding crop and seasonal effects influence fungal, bacterial and nematode diversity in wheat and oilseed rape rhizosphere and soil. Applied Soil Ecology 126, 34–46. https://doi.org/10.1016/j.apsoil.2018.02.007.

Hoang, D.T.T., Rashtbari, M., Anh, L.T., Wang, S., Tu, D.T., Hiep, N.V., Razavi, B.S., 2022. Mutualistic interaction between arbuscular mycorrhiza fungi and soybean roots enhances drought resistant through regulating glucose exudation and rhizosphere expansion. Soil Biology and Biochemistry 171, 108728. https://doi.org/10.1016/J.SOILBIO.2022.108728.

Joergensen, R.G., 1996. The fumigation-extraction method to estimate soil microbial biomass: calibration of the kEC value. Soil Biology and Biochemistry 28, 25–31. https://doi.org/10.1016/0038-0717(95)00102-6.

Jones, P., Garcia, B.J., Furches, A., Tuskan, G.A., Jacobson, D., 2019. Plant host-associated mechanisms for microbial selection. Frontiers in Plant Science 10, 1–14. https://doi.org/10.3389/fpls.2019.00862.

Kaloterakis, N., van Delden, S.H., Hartley, S., De Deyn, G.B., 2021. Silicon application and plant growth promoting rhizobacteria consisting of six pure *Bacillus* species alleviate salinity stress in cucumber (*Cucumis sativus* L). Scientia Horticulturae 288, 110383. https://doi.org/10.1016/J.SCIENTA.2021.110383.

Kerdraon, L., Balesdent, M.-H., Barret, M., Laval, V., Suffert, F., 2019. Crop residues in wheat-oilseed rape rotation system: a pivotal, shifting platform for microbial meetings. Microbial Ecology 77, 931–945. https://doi.org/10.1007/s00248-019-01340-8.

Kelly, C., Haddix, M.L., Byrne, P.F., Cotrufo, M.F., Schipanski, M., Kallenbach, C.M., Wallenstein, M.D., Fonte, S.J., 2022. Divergent belowground carbon allocation patterns of winter wheat shape rhizosphere microbial communities and nitrogen cycling activities. Soil Biology and Biochemistry 165, 108518. https://doi.org/10.1016/j.soilbio.2021.108518.

Kirkegaard, J., Christen, O., Krupinsky, J., Layzell, D., 2008. Break crop benefits in temperate wheat production. Field Crops Research 107, 185–195. https://doi.org/10.1016/j.fcr.2008.02.010.

Korenblum, E., Dong, Y., Szymanski, J., Panda, S., Jozwiak, A., Massalha, H., Meir, S., Rogachev, I., Aharoni, A., 2020. Rhizosphere microbiome mediates systemic root metabolite exudation by root-to-root signaling. Proceedings of the National Academy of Sciences of the United States of America 117, 3874–3883. https://doi.org/10.1073/pnas.1912130117.

Kramer-Walter, K.R., Bellingham, P.J., Millar, T.R., Smissen, R.D., Richardson, S.J., Laughlin, D.C., 2016. Root traits are multidimensional: specific root length is independent from root tissue density and the plant economic spectrum. Journal of Ecology 104, 1299–1310. https://doi.org/10.1111/1365-2745.12562.

Kuzyakov, Y., Jones, D.L., 2006. Glucose uptake by maize roots and its transformation in the rhizosphere. Soil Biology and Biochemistry 38, 851–860. https://doi.org/10.1016/j.soilbio.2005.07.012.

Kuzyakov, Y., Domanski, G., 2000. Carbon input by plants into the soil. Review. Journal of Plant Nutrition and Soil Science 163, 421–431. https://doi.org/10.1002/1522-2624(200008)163:4<421::AID-JPLN421>3.0.CO;2-R.

Kuzyakov, Y., Razavi, B.S., 2019. Rhizosphere size and shape: temporal dynamics and spatial stationarity. Soil Biology and Biochemistry 135, 343–360. https://doi.org/10.1016/j.soilbio.2019.05.011.

Kuzyakov, Y., Xu, X., 2013. Competition between roots and microorganisms for nitrogen: mechanisms and ecological relevance. New Phytologist 198, 656–669. https://doi.org/10.1111/nph.12235.

Kwak, Y.S., Weller, D.M., 2013. Take-all of wheat and natural disease suppression: a review. Plant Pathology Journal 29, 125–135. https://doi.org/10.5423/PPJ.SI.07.2012.0112.

Lahti, L., Shetty, S., et al., 2017. Microbiome: tools for microbiome analysis in R. Version. Available at: https://github.com/microbiome/microbiome/.

Lange, M., Eisenhauer, N., Sierra, C.A., Bessler, H., Engels, C., Griffiths, R.I., Mellado-Vázquez, P.G., Malik, A.A., Roy, J., Scheu, S., Steinbeiss, S., Thomson, B.C., Trumbore, S.E., Gleixner, G., 2015. Plant diversity increases soil microbial activity and soil carbon storage. Nature Communications 6, 6707. https://doi.org/10.1038/ncomms7707.

Lopez, G., Ahmadi, S.H., Amelung, W., Athmann, M., Ewert, F., Gaiser, T., Gocke, M.I., Kautz, T., Postma, J., Rachmilevitch, S., Schaaf, G., Schnepf, A., Stoschus, A., Watt, M., Yu, P., Seidel, S.J., 2023. Nutrient deficiency effects on root architecture and root-to-shoot ratio in arable crops. Frontiers in Plant Science 13, 1–18. https://doi.org/10.3389/fpls.2022.1067498.

Luan, H., Liu, Y., Huang, S., Qiao, W., Chen, J., Guo, T., Zhang, Xiaojia, Guo, S., Zhang, Xuemei, Qi, G., 2022. Successive walnut plantations alter soil carbon quantity and quality by modifying microbial communities and enzyme activities. Frontiers in Microbiology 13, 1–14. https://doi.org/10.3389/fmicb.2022.953552.

Ma, X., Zarebanadkouki, M., Kuzyakov, Y., Blagodatskaya, E., Pausch, J., Razavi, B.S., 2018. Spatial patterns of enzyme activities in the rhizosphere: effects of root hairs and root radius. Soil Biology and Biochemistry 118, 69–78. https://doi.org/10.1016/J.SOILBIO.2017.12.009.

Mayer, Z., Sasvári, Z., Szentpéteri, V., Rétháti, B.P., Vajna, B., Posta, K., 2019. Effect of long-term cropping systems on the diversity of the soil bacterial communities. Agronomy 9, 1–10. https://doi.org/10.3390/agronomy9120878.

McMurdie, P.J., Holmes, S., 2013. Phyloseq: an R package for reproducible interactive analysis and graphics of microbiome census data. PLoS One 8, e61217. https://doi.org/10.1371/journal.pone.0061217.

Meier, I.C., Finzi, A.C., Phillips, R.P., 2017. Root exudates increase N availability by stimulating microbial turnover of fast-cycling N pools. Soil Biology and Biochemistry 106, 119–128. https://doi.org/10.1016/j.soilbio.2016.12.004.

Mohan, S., Kiran Kumar, K., Sutar, V., Saha, S., Rowe, J., Davies, K.G., 2020. Plant root-exudates recruit hyperparasitic bacteria of phytonematodes by altered cuticle aging: implications for biological control strategies. Frontiers in Plant Science 11, 763. https://doi.org/10.3389/fpls.2020.00763.

Näsholm, T., Kielland, K., Ganeteg, U., 2009. Uptake of organic nitrogen by plants. New Phytologist 182, 31–48. https://doi.org/10.1111/j.1469-8137.2008.02751.x.

Ni, X., Liao, S., Tan, S., Peng, Y., Wang, D., Yue, K., Wu, F., Yang, Y., 2020. The vertical distribution and control of microbial necromass carbon in forest soils. Global Ecology and Biogeography 29, 1829–1839. https://doi.org/10.1111/geb.13159.

Oksanen, J., Kindt, R., Legendre, P., O'Hara, B., Simpson, G.L., Solymos, P., Stevens, M.H.H., Wagner, H., 2020. Vegan: community ecology package. Available at: https://CRAN.R-project.org/package=vegan.

Palma-Guerrero, J., Chancellor, T., Spong, J., Canning, G., Hammond, J., McMillan, V.E., Hammond-Kosack, K.E., 2021. Take-all disease: new insights into an important wheat root pathogen. Trends in Plant Science 26, 836–848. https://doi.org/10.1016/j.tplants.2021.02.009.

Pang, Z., Chen, J., Wang, T., Gao, C., Li, Z., Guo, L., Xu, J., Cheng, Y., 2021. Linking plant secondary metabolites and plant microbiomes: a review. Frontiers in Plant Science 12, 621276. https://doi.org/10.3389/fpls.2021.621276.

Panikov, N.S., Blagodatsky, S.A., Blagodatskaya, J.V., Glagolev, M.V., 1992. Determination of microbial mineralization activity in soil by modified Wright and Hobbie method. Biology and Fertility of Soils 14, 280–287. https://doi.org/10.1007/BF00395464.

Pascault, N., Cécillon, L., Mathieu, O., Hénault, C., Sarr, A., Lévêque, J., Farcy, P., Ranjard, L., Maron, P.A., 2010. In situ dynamics of microbial communities during decomposition of wheat, rape, and alfalfa residues. Microbial Ecology 60, 816–828. https://doi.org/10.1007/s00248-010-9705-7.

Paungfoo-Lonhienne, C., Lonhienne, T.G.A., Rentsch, D., Robinson, N., Christie, M., Webb, R.I., Gamage, H.K., Carroll, B.J., Schenk, P.M., Schmidt, S., 2008. Plants can use protein as a nitrogen source without assistance from other organisms. Proceedings of the National Academy of Sciences of the United States of America 105, 4524–4529. https://doi.org/10.1073/pnas.0712078105.

Pausch, J., Kuzyakov, Y., 2017. Carbon input by roots into the soil: quantification of rhizodeposition from root to ecosystem scale. Global Change Biology 24, 1–12. https://doi.org/10.1111/gcb.13850.

Philippot, L., Raaijmakers, J.M., Lemanceau, P., Van Der Putten, W.H., 2013. Going back to the roots: the microbial ecology of the rhizosphere. Nature Reviews Microbiology 11, 789–799. https://doi.org/10.1038/nrmicro3109.

Pivato, B., Semblat, A., Guégan, T., Jacquiod, S., Martin, J., Deau, F., Moutier, N., Lecomte, C., Burstin, J., Lemanceau, P., 2021. Rhizosphere bacterial networks, but not diversity, are impacted by pea-wheat intercropping. Frontiers in Microbiology 12, 1–13. https://doi.org/10.3389/fmicb.2021.674556.

Qi, B., Zhang, K., Qin, S., Lyu, D., He, J., 2022. Glucose addition promotes C fixation and bacteria diversity in C-poor soils, improves root morphology, and enhances key N metabolism in apple roots. PLoS One 17, e0262691.

Quast, C., Pruesse, E., Yilmaz, P., Gerken, J., Schweer, T., Yarza, P., Peplies, J., Glöckner, F.O., 2013. The SILVA ribosomal RNA gene database project: improved data processing and web-based tools. Nucleic Acids Research 41, 590–596. https://doi.org/10.1093/nar/gks1219.

R Core Team, 2016. R: a Language and Environment for Statistical Computing. R Foundation for Statistical Computing, Vienna, Austria.

Ramanauskienė, J., Semaškienė, R., Jonavičienė, A., Ronis, A., 2018. The effect of crop rotation and fungicide seed treatment on take-all in winter cereals in Lithuania. Crop Protection 110, 14–20. https://doi.org/10.1016/j.cropro.2018.03.011.

Razavi, B.S., Zarebanadkouki, M., Blagodatskaya, E., Kuzyakov, Y., 2016. Rhizosphere shape of lentil and maize: spatial distribution of enzyme activities. Soil Biology and Biochemistry 96, 229–237. https://doi.org/10.1016/J.SOILBIO.2016.02.020.

Razavi, B.S., Zhang, X., Bilyera, N., Guber, A., Zarebanadkouki, M., 2019. Soil zymography: simple and reliable? Review of current knowledge and optimization of the method. Rhizosphere 11, 100161. https://doi.org/10.1016/J.RHISPH.2019.100161.

Reichel, R., Kamau, C.W., Kumar, A., Li, Z., Radl, V., Temperton, V.M., Schloter, M., Brüggemann, N., 2022. Spring barley performance benefits from simultaneous shallow straw incorporation and top dressing as revealed by rhizotrons with resealable sampling ports. Biology and Fertility of Soils 58, 375–388. https://doi.org/10.1007/s00374-022-01624-1.

Ren, C., Chen, J., Deng, J., Zhao, F., Han, X., Yang, G., Tong, X., Feng, Y., Shelton, S., Ren, G., 2017. Response of microbial diversity to C:N:P stoichiometry in fine root and microbial biomass following afforestation. Biology and Fertility of Soils 53, 457–468. https://doi.org/10.1007/s00374-017-1197-x.

Rillig, M.C., Caldwell, B.A., Wösten, H.A.B., Sollins, P., 2007. Role of proteins in soil carbon and nitrogen storage: controls on persistence. Biogeochemistry 85, 25–44. https://doi.org/10.1007/s10533-007-9102-6.

Rose, L., 2017. Pitfalls in root trait calculations: how ignoring diameter heterogeneity can lead to overestimation of functional traits. Frontiers in Plant Science 8, 1–5. https://doi.org/10.3389/fpls.2017.00898.

Shi, Y., Sheng, L., Wang, Z., Zhang, X., He, N., Yu, Q., 2016. Responses of soil enzyme activity and microbial community compositions to nitrogen addition in bulk and microaggregate soil in the temperate steppe of Inner Mongolia. Eurasian Soil Science 49, 1149–1160. https://doi.org/10.1134/S1064229316100124.

Schreiter, S., Ding, G.-C., Heuer, H., Neumann, G., Sandmann, M., Grosch, R., Kropf, S., Smalla, K., 2014. Effect of the soil type on the microbiome in the rhizosphere of field-grown lettuce. Frontiers in Microbiology 5, 144. https://doi.org/10.3389/fmicb.2014.00144.

Sieling, K., 2005. Growth stage-specific application of slurry and mineral N to oilseed rape, wheat and barley. Journal of Agricultural Science 142, 495–502. https://doi.org/10.1017/S0021859604004757.

Sieling, K., Christen, O., 2015. Crop rotation effects on yield of oilseed rape, wheat and barley and residual effects on the subsequent wheat. Archives of Agronomy and Soil Science 61, 1531–1549. https://doi.org/10.1080/03650340.2015.1017569.

Singh, G., Verman, A.K., Kumar, V., 2016. Catalytic properties, functional attributes and industrial applications of b -glucosidases. 3 Biotech 6, 1–14. https://doi.org/10.1007/s13205-015-0328-z.

Smagacz, J., Kozieł, M., Martyniuk, S., 2016. Soil properties and yields of winter wheat after long-term growing of this crop in two contrasting rotations. Plant Soil and Environment 62, 566–570. https://doi.org/10.17221/582/2016-PSE.

Song, X., Razavi, B.S., Ludwig, B., Zamanian, K., Zang, H., Kuzyakov, Y., Dippold, M.A., Gunina, A., 2020. Combined biochar and nitrogen application stimulates enzyme activity and root plasticity. Science of the Total Environment 735, 139393. https://doi.org/10.1016/j.scitotenv.2020.139393.

Spitzer, C.M., Lindahl, B., Wardle, D.A., Sundqvist, M.K., Gundale, M.J., Fanin, N., Kardol, P., 2021. Root trait–microbial relationships across tundra plant species. New Phytologist 229, 1508–1520. https://doi.org/10.1111/nph.16982.

Town, J.R., Dumonceaux, T., Tidemann, B., Helgason, B.L., 2023. Crop rotation significantly influences the composition of soil, rhizosphere, and root microbiota in canola (*Brassica napus* L.). Environmental Microbiome 18, 1–14. https://doi.org/10.1186/s40793-023-00495-9.

Turner, B.L., Hopkins, D.W., Haygarth, P.M., Ostle, N., 2002. β-Glucosidase activity in pasture soils. Applied Soil Ecology 20, 157–162. https://doi.org/10.1016/S0929-1393(02)00020-3.

Veres, Z., Kotroczó, Z., Fekete, I., Tóth, J.A., Lajtha, K., Townsend, K., Tóthmérész, B., 2015. Soil extracellular enzyme activities are sensitive indicators of detrital inputs and carbon availability. Applied Soil Ecology 92, 18–23. https://doi.org/10.1016/j.apsoil.2015.03.006.

Vlot, A.C., Sales, J.H., Lenk, M., Bauer, K., Brambilla, A., Sommer, A., Chen, Y., Wenig, M., Nayem, S., 2020. Systemic propagation of immunity in plants. New Phytologist 229, 1234–1250. https://doi.org/10.1111/nph.16953.

Vujanovic, V., Mavragani, D., Hamel, C., 2012. Fungal communities associated with durum wheat production system: a characterization by growth stage, plant organ and preceding crop. Crop Protection 37, 26–34. https://doi.org/10.1016/j.cropro.2012.02.006.

Weiser, C., Fuß, R., Kage, H., Flessa, H., 2018. Do farmers in Germany exploit the potential yield and nitrogen benefits from preceding oilseed rape in winter wheat cultivation? Archives of Agronomy and Soil Science 64, 25–37. https://doi.org/10.1080/03650340.2017.1326031.

Wen, T., Yu, G.H., Hong, W.D., Yuan, J., Niu, G.Q., Xie, P.H., Sun, F.S., Guo, L.D., Kuzyakov, Y., Shen, Q.R., 2022. Root exudate chemistry affects soil carbon mobilization via microbial community reassembly. Fundamental Research 2, 697–707. https://doi.org/10.1016/j.fmre.2021.12.016.

Woo, S.L., De Filippis, F., Zotti, M., Vandenberg, A., Hucl, P., Bonanomi, G., 2022. pea-wheat rotation affects soil microbiota diversity, community structure, and soil borne Pathogens. Microorganisms 10, 370. https://doi.org/10.3390/microorganisms10020370.

Wu, J., Joergensen, R.G., Pommerening, B., Chaussod, R., Brookes, P.C., 1990. Measurement of soil microbial biomass C by fumigation-extraction—an automated procedure. Soil Biology and Biochemistry 22, 1167–1169. https://doi.org/10.1016/0038-0717(90)90046-3.

Yahya, M., Islam, E. ul, Rasul, M., Farooq, I., Mahreen, N., Tawab, A., Irfan, M., Rajput, L., Amin, I., Yasmin, S., 2021. Differential root exudation and architecture for improved growth of wheat mediated by phosphate solubilizing bacteria. Frontiers in Microbiology 12, 1–23. https://doi.org/10.3389/fmicb.2021.744094.

Yang, Y., Li, M., Wu, J., Pan, X., Gao, C., Tang, D.W.S., 2022. Impact of combining long-term subsoiling and organic fertilizer on soil microbial biomass carbon and nitrogen, soil enzyme activity, and water use of winter wheat. Frontiers in Plant Science 12, 1–13. https://doi.org/10.3389/fpls.2021.788651.

Yeo, I.N.K., Johnson, R.A., 2000. A new family of power transformations to improve normality or symmetry. Biometrika 87, 954–959. https://doi.org/10.1093/biomet/87.4.954.

Yin, C., Schlatter, D., Hagerty, C., Hulbert, S., Paulitz, T.C., 2022. Disease-induced assemblage of the rhizosphere fungal community in successive plantings of wheat. Phytobiomes Journal. https://doi.org/10.1094/pbiomes-12-22-0101-r.

Yuan, L., Gao, Y., Mei, Y., Liu, J., Kalkhajeh, Y.K., Hu, H., Huang, J., 2023. Effects of continuous straw returning on bacterial community structure and enzyme activities in rape-rice soil aggregates. Scientific Reports 13, 2357. https://doi.org/10.1038/s41598-023-28747-1.

Zhao, S., Zhang, S., 2018. Linkages between straw decomposition rate and the change in microbial fractions and extracellular enzyme activities in soils under different long-term fertilization treatments. PLoS One 13, e0202660. https://doi.org/10.1371/journal.pone.0202660.

Zhang, X., Kuzyakov, Y., Zang, H., Dippold, M.A., Shi, L., Spielvogel, S., Razavi, B.S., 2020. Rhizosphere hotspots: root hairs and warming control microbial efficiency, carbon utilization and energy production. Soil Biology and Biochemistry 148, 107872. https://doi.org/10.1016/j.soilbio.2020.107872.

Zhou, M., Diwu, Z., Panchuk-Voloshina, N., Haugland, R.P., 1997. A stable nonfluorescent derivative of resorufin for the fluorometric determination of trace hydrogen peroxide: applications in detecting the activity of phagocyte NADPH oxidase and other oxidases. Analytical Biochemistry 253, 162–168. https://doi.org/10.1006/ABIO.1997.2391.

Kavamura, V.N., Robinson, R.J., Hughes, D., Clark, I., Rossmann, M., de Melo, I.S., Hirsch, P.R., Mendes, R., Mauchline, T.H., 2020. Wheat dwarfing influences selection of the rhizosphere microbiome. Scientific Reports 10, 1–11. https://doi.org/10.1038/s41598-020-58402-y.

Kielak, A.M., Barreto, C.C., Kowalchuk, G.A., van Veen, J.A., Kuramae, E.E., 2016. The ecology of Acidobacteria: Moving beyond genes and genomes. Frontiers in Microbiology 7, 744. https://doi.org/10.3389/fmicb.2016.00744.